EUROPEAN ORGANIZATION FOR NUCLEAR RESEARCH

DIRAC Note 2015-03
May 29, 2015

Production rates for π^+K^-, π^-K^+ and $\pi^+\pi^-$ atoms in p-Ni interactions at proton momentum 24 and 450 GeV/c.

O.Gorchakov, L.Nemenov

GENEVA
2015

Abstract

The results of performed analysis show that the yield of π^+K^-, $K^+\pi^-$ and $\pi^+\pi^-$ atoms in the p-nucleus interactions increases significantly at change of proton momentum P_p from 24 up to 450 GeV/c. The yield of these dimesoatoms at $P_p =$ 450 GeV/c and $\theta_{lab} = 4^\circ$ is more than on the order of magnitude more than the one at DIRAC experiment conditions: $P_p = 24$ GeV/c and $\theta_{lab} = 5.7^\circ$. The large yield of dimesoatoms allows to improve their lifetime measurement and to investigate long-lived $\pi^+\pi^-$ atoms significantly.

1 Introduction

The lifetime measurement of atoms consisting of π^+ and $\pi^-(A_{2\pi})$, K^+ and $\pi^-(A_{K\pi})$ and K^- and $\pi^+(A_{\pi K})$ allows to measure by model independent way the $\pi\pi$ and $K\pi$ scattering lengths [1, 2, 3, 4]. The experimental investigation of $A_{2\pi}$ and search for $K\pi$ atoms were done using PS CERN proton beam with momentum $P_p = 24$ GeV/c. The lifetime of $A_{2\pi}$ was measured in [5, 6] with precision about 9% which gives for the $\pi\pi$ scattering lengths $|a_0 - a_2|$ accuracy 4,3% (statistical error 3.1%) which is far away from the theoretical predictions 1.5% [3]. The limited number of produced and detected $K\pi$ atoms allowed to evaluate the value of $K\pi$ atom lifetime and $K\pi$ scattering lengths $|a_{1/2} - a_{3/2}|$ with precision 100% and 60% accordingly [7]. The theoretical prediction precisions for the $K\pi$ atom life time and $K\pi$ scattering length values are the 10% and 5% accordingly [8, 9, 10, 11].

The investigation of $A_{2\pi}$ allows also to measure the Lamb shift in this atom [12, 13, 14] and to extract the another combination of $\pi\pi$ scattering lengths $2a_0 + a_2$. If the resonance method can be used then this combination will be extracted with precision on the order higher than accuracy of other methods[15, 16]. At the present time in the DIRAC experiment 436±61 long-lived $A_{2\pi}$ were observed with statistical error ±57([17]).

It is obvious that for the investigation of $K\pi$ atoms, $\pi\pi$ atom Lamb shift measurement and lifetime accuracy improvement the detected number of atoms must be enlarged more than on the order. The dimesoatom yield large increasing with growth of P_p from 24 GeV/c up to 450 GeV/c was established in [18, 19, 20]. In [20] the yields and spectra of $A_{2\pi}$, $A_{\pi^+K^-}$ and $A_{\pi^-K^+}$ generated in p-Ni interaction at $P_p = 24$ and 450 GeV/c were calculated a bit precisely than in [18, 19]. Because the yields of $A_{2\pi}$, $A_{\pi^+K^-}$ and $A_{\pi^-K^+}$ at $P_p = 24$ GeV/c and $\theta_{lab} = 5.7^\circ$ are measured now, the ratio of these atom yields at $P_p = 450$ GeV/c, $\theta_{lab} = 0 \div 5.7^\circ$ and at $P_p = 24$ GeV/c were calculated. It allows to determine the optimal value of θ_{lab} at 450 GeV/c and expected statistics of $A_{2\pi}$ and $A_{\pi K}$.

In [20] to obtain the yields of $K^{\pm}$- and $\pi^{\pm}$-mesons the computer simulation programs FRITIOF 6.0 and JETSET 7.3 [21] (CERN Program Library) based on the Lund string fragmentation model was used. FRITIOF is a generator for hadron-hadron, hadron-nucleus and nucleus-nucleus collisions, which makes use of JETSET for fragmentation.

In the present work the same calculations were performed using FTF generator [22] - the developed version of FTITIOF generator for GEANT4[23]. Experimental data on K^+, K^-, π^+ and π^- production inclusive cross sections at proton momentum 31 GeV/c(p-C)[24] and 450 GeV/c(p-Be)[25] were compared with the generator predictions. The experimental inclusive cross section of K^+, K^-, π^+ and π^- in the angular and momentum intervals coinciding with the intervals of the DIRAC experiment were used to evaluate the FTF precision at P_p =31 GeV/c. This precision was used as a accuracy of FTF description of the same cross sections at 24 GeV/c. The FTF accuracy at 450 GeV/c was checked only in the laboratory angle interval $0 \div 1.7^{\circ}$. The dimesoatom yields at 450 GeV/c as a function of θ_{lab} and atom momentum were calculated. It allows to obtain the statistical precision of $A_{\pi K}$ lifetime measurement and to determine the possible accuracy of the Lamb shift of $A_{2\pi}$ measurement. Also the experimental data from p-C and p-Cu interactions at proton momentum 100 GeV/c[26] were compared with the generator predictions to make the conclusion about FTF possibility to describe inclusive cross sections on both nuclei.

2 Basic relations

The probability of atom production is proportional to the double inclusive cross section for generation of the two constituent particles of this atom with small relative momenta. Calculating the atom production cross section, one should exclude the contribution to the double cross section from those constituents that arise from the decays of long-lived particles and can not form the atom. When one or both particles in the pair come from these decays, the typical range between them is much larger than the Bohr radius of the atom (387 fm for $A_{2\pi}$ and 249 fm for$A_{\pi K}$) and the probability of atom production is negligible. The main long-lived sources of pions are η and η'. For the case of pions and kaons the short-lived sources constitute the main contribution.

The laboratory differential inclusive cross section for the atom production can be written in the form [12]

$$\frac{d\sigma_n^A}{d\vec{p}_A} = (2\pi)^3 \frac{E_A}{M_A} |\Psi_n(0)|^2 \left. \frac{d^2\sigma_s}{d\vec{p}_1\, d\vec{p}_2} \right|_{\vec{p}_1=\frac{m_1}{m_2}\vec{p}_2=\frac{m_1}{M_A}\vec{p}_A}, \qquad (1)$$

where M_A is the atom mass, $\vec{p}_A$ and E_A are the momentum and energy of the atom in the lab system, respectively, $|\Psi_n(0)|^2 = p_B^3/\pi n^3$ is the atomic wave function (without regard for the strong interactions between the particles forming the atom, i.e. the pure Coulomb wave function) squared at the origin with the principal quantum number n and the orbital momentum $l = 0$, p_B is the Bohr momentum of the particles in the atom, $d^2\sigma_s^0/d\vec{p}_1 d\vec{p}_2$ is the double inclusive production cross section for the pairs from short-lived sources (hadronization processes, ρ, ω, Δ, K^*, Σ^*, etc.) without regard for the $\pi^+\pi^-$ ($K^+\pi^-$, $K^-\pi^+$) Coulomb interaction in the final state, $\vec{p}_1$ and $\vec{p}_2$ are the momenta of the particles forming the atom in the lab system. The momenta obey the relation $\vec{p}_1 = \frac{m_1}{m_2}\vec{p}_2 = \frac{m_1}{M_A}\vec{p}_A$ (m_1 and m_2 are the masses of the particles). The atoms are produced with the orbital momentum $l = 0$, because $|\Psi_{n,l}(0)|^2 = 0$ when $l \neq 0$. The atoms are

distributed over n as n^{-3}: $W_1 = 83\%$, $W_2 = 10.4\%$, $W_3 = 3.1\%$, $W_{n\geq 4} = 3.5\%$. Note that $\Sigma_{n=1}^{\infty}|\Psi_n(0)|^2 = 1.202|\Psi_1(0)|^2$.

After substituting the expression for $|\Psi_n(0)|^2$ and summing over n, one can obtain an expression for the inclusive yield of atoms in all S-states through the inclusive yields of positive and negative hadron pairs

$$\frac{d\sigma^A}{d\vec{p}_A} = 1.202 \cdot 8\,\pi^2\,(\mu\alpha)^3\,\frac{E_A}{M_A}\,\left.\frac{d^2\sigma_s}{d\vec{p}_1\,d\vec{p}_2}\right|_{\vec{p}_1=\frac{m_1}{m_2}\vec{p}_2=\frac{m_1}{M_A}\vec{p}_A}, \qquad (2)$$

where μ is the reduced mass of the atom ($\mu = \frac{m_1 m_2}{m_1+m_2}$), α is the fine structure constant.

Instead of differential cross section it is convenient to introduce the probability of particle production per one inelastic interaction (yield):

$$\frac{dN}{d\vec{p}} = \frac{d\sigma}{d\vec{p}}\,\frac{1}{\sigma_{in}}, \qquad \frac{d^2N}{d\vec{p_1}d\vec{p_2}} = \frac{d^2\sigma}{d\vec{p_1}d\vec{p_2}}\,\frac{1}{\sigma_{in}}, \qquad (3)$$

where σ_{in} is the inelastic cross section of hadron production.

Then

$$\frac{dN_A}{d\vec{p}_A} = 1.202 \cdot 8\,\pi^2\,(\mu\alpha)^3\,\frac{E_A}{M_A}\,\left.\frac{d^2N_s}{d\vec{p}_1\,d\vec{p}_2}\right|_{\vec{p}_1=\frac{m_1}{m_2}\vec{p}_2=\frac{m_1}{M_A}\vec{p}_A}, \qquad (4)$$

The double yield(without regard for the Coulomb interaction) can be presented as [27]:

$$\frac{d^2N_s}{d\vec{p}_1 d\vec{p}_2} = \frac{dN_1}{d\vec{p}_1}\,\frac{dN_2}{d\vec{p}_2}\,R(\vec{p_1},\vec{p_2},S), \qquad (5)$$

where $dN_1/d\vec{p}_1$ and $dN_2/d\vec{p}_2$ are the single particle yields, R is a correlation function due to strong interaction only and S is the square of full c.m.s. energy of beam proton and target hadron.

The yield and momentum distribution of $A_{2\pi}$ atoms were measured at $P_p = 24$ GeV/c[6] and $\theta_{lab} = 5.7^\circ$, the yields of π^+K^- and $K^+\pi^-$ atoms at the same momentum and angle were obtained in [7]. Hence it is useful to present not only the absolute yields of atoms at different conditions but their yields relative to the known values.

3 Experimental values of pion and kaon inclusive cross sections and their description by FTF.

It is important to know how well the inclusive cross sections obtained by FTF coincide with corresponding experimental data. In the case of $A_{2\pi}$ atoms the main interval of pion momentum is $1 \div 3$ GeV/c and for kaons from $A_{\pi K}$ is $4 \div 7$ GeV/c. We are going to use Ni target but there is no data for pion and kaon inclusive cross sections for such material. The data [28] reveals the weak dependence of soft pion and kaon yields on the nucleon atomic number A from Be up to Cu. Also there is the weak dependence of these yields on A in p-nucleus (C, Al, Cu) interactions at $P_p = 100$ GeV/c for the secondary particle momentum 30 GeV/c[26]. Therefore the values of soft dimesoatom yields calculated and measured for p-Ni interactions are a good estimation of the same yields in any p-nucleus interaction.

3.1 Comparison of experimental inclusive cross sections in p-C interactions at Pp = 31 GeV/c with FTF predictions.

The inclusive cross sections of π^+, π^-, K^+ and K^- in p-C interactions at $P_p = 31$ GeV/c. were measured [24] with high precision and compared with VENUS, EPOS and GiBUU predictions.

The Fig.1-8 present the experimental and calculated inclusive yield values of π^+, π^-, K^+ and K^- as a function of particle momentum in l.s.. The intervals of π^+ and π^- polar angle θ_{lab} in l.s. from 60÷100 $mrad$ and 100÷140 $mrad$ fully cover the θ_{lab} interval of the DIRAC setup (82÷116 $mrad$). From Fig.2 and 3 we can see that the FTF describes the inclusive cross sections in the momentum interval 1÷3 GeV/c better than 10%.

For K^+ inclusive yields in wide θ_{lab} interval 20÷140 $mrad$ (Fig.6) the calculated values are on 30% higher than experimental ones. But in the θ_{lab} interval 140÷240 $mrad$ (Fig.6) where P_t are relatively large the agreement is good. Therefore it is possible that the FTF is describing the experimental data in the interval 82÷116 $mrad$ with relatively high P_t better than in the hole interval 20÷140 $mrad$. In this case the 30% precision is the upper limit of the inclusive cross section uncertainty.

For K^- in the interval 60÷140 $mrad$ the calculated values higher than experimental data (Fig.7,8) on $\approx$ 15 % at P_K =4 GeV/c and on $\approx$ 100 % at P_K = 7 GeV/c.

3.2 Comparison of experimental inclusive cross sections in p-nucleus interactions at P_p = 450 GeV/c with FTF predictions.

The invariant inclusive cross sections of π^+, π^-, K^+ and K^- in p-Be interactions at P_p = 450 GeV/c were measured [25] and presented for $\theta_{lab} = 0^\circ$ together with FTF calculations on Fig.9. It follows that the generator describes the inclusive cross sections of π^+ up to momentum 40 GeV/c , π^- up to 70 GeV/c. Therefore generator can be used for description of $A_{2\pi}$ up to momentum 80 GeV/c.

The inclusive cross sections of K mesons are described with precision about 20% up to momentum 20 GeV/c and 40 GeV/c for K^+ and K^- accordingly. It allows to calculate the yields of $A_{K\pi}$ and $A_{\pi K}$ up to momentum 26 GeV/c and 51 GeV/c accordingly.

The dependence of experimental inclusive yields of π and K mesons with $P = 15$ GeV/c and $P = 40$ GeV/c on P_t is presented on Fig.10 together with FTF predictions. There is a good agreement demonstrating that generator describes well the inclusive cross section angular dependence up to $\theta_{lab} = 1.7^\circ$ and can be used at greater θ_{lab} values.

3.3 Comparison of experimental inclusive cross sections in p-nucleus interactions at P_p = 100 GeV/c with FTF predictions.

The data on inclusive production of π^+, π^-, K^+ and K^- in p-C and p-Cu interactions at $P_p = 100$ GeV/c were measured [26] and presented on Fig.11-14 as a function of transverse momentum together with FTF calculations.

The conclusion is that the FTF does not describe experimental data at large values of x for C. The discrepancy of FTF predictions and p-Cu experimental data is less. It can

be considered as the indication that the yield of dimesoatoms at P_p = 450 GeV/c from Ni target can be described by FTF better than from Be target.

4 Results of calculations

The selection of particles from long-lived and short-lived sources was performed. Further, using yields from the short-lived sources only we obtained the double inclusive yields of $\pi^+\pi^-$, $K^+\pi^-$ and $K^-\pi^+$ pairs and the distributions of corresponding atom yields over the angle and momentum in l.s..

4.1 The calculations of inclusive yields of all charged particles, $\pi\pi$ and πK atoms.

On the Fig.15 the total yields of charged particles ($\pi^\pm$, $K^\pm$, p and $\bar{p}$) per one p-Ni interaction at the proton momentum 450 GeV/c and emission angles $\theta_{lab} = 0°$, $2°$, $4°$(bottom) and at the proton momentum 24 GeV/c and emission angle $\theta_{lab} = 5.7°$(top) as a function of their momentum for solid angle of 10^{-3} sr are shown.

On the Fig.16 there are the yields of atoms for solid angle of 10^{-3} sr and without any constrains on atom momentum without taking into account the decays of pions and kaons along the setup.

On Fig.17 the yields of $A_{2\pi}$, $A_{\pi^+K^-}$ and $A_{K^+\pi^-}$ per one p-Ni interaction at the proton momentum 450 GeV/c and emission angles $\theta_{lab} = 0°$, $2°$, $4°$ and at the proton momentum 24 GeV/c and emission angle $\theta_{lab} = 5.7°$ as a function of these atom momentum P_A are presented in the intervals 2.5÷10.5 GeV/c($A_{2\pi}$) and 5÷14 GeV/c ($A_{\pi K}$) without taking into account the decays of pions and kaons in the setup. The chosen intervals are the working intervals of DIRAC setup. In the Tab.1 these yields integrated over P_A are shown where W_{ch} and W_A are the total yields of charged particles ($\pi^\pm$, $K^\pm$, p, $\bar{p}$) and $\pi^+\pi^-$, π^+K^-, $K^+\pi^-$ atoms accordingly into the aperture of 10^{-3} sr per one p-Ni interaction. The relative yields of charged particles and atoms are W^N_{ch}=$W_{ch}/W_{ch}(5.7°, 24\ GeV/c)$ and W^N_A=$W_A/W_A(5.7°, 24\ GeV/c)$).

At $\theta_{lab} = 4°$ and P_p=450 GeV/c the yields of $\pi^+\pi^-$, π^+K^- and $K^+\pi^-$ atoms are in 17, 37 and 16 times more respectively , than at $\theta_{lab} = 5.7°$ and P_p=24 GeV/c.

4.2 Calculations of inclusive yields of $\pi^+\pi^-$ and πK atoms detected by setup

Here we take into account the DIRAC setup acceptance (Fig.18) and pion and kaon decays also.

On Fig.19 the yields of $A_{2\pi}$, $A_{\pi^+K^-}$ and $A_{K^+\pi^-}$ per one p-Ni interaction in solid angle 10^{-3} sr at the proton momentum 450 GeV/c, emission angles $\theta_{lab} = 0°$, $2°$, $4°$ and at the proton momentum 24 GeV/c and emission angle $\theta_{lab} = 5.7°$ as a function of these atom momentum with taking into account the acceptance of setup are presented. In the Tab.2 these yields integrated over P_A are shown. There are shown the absolute values of atomic yields, their relative values when their yield at 24 GeV/c and 5.7° is set to 1 and their values relative to the flux of charged particles in the DIRAC channel. The last values are important as in the channel there are the forward detectors which should operate at this

Table 1: The total yield of charged particles ($\pi^{\pm}$, $K^{\pm}$, p and $\bar{p}$) W_{ch}, $\pi^+\pi^-$, π^+K^- and $K^+\pi^-$ atoms W_A into the aperture of 10^{-3} sr per one p-Ni interaction at the proton momenta P_p = 24 and 450 GeV/c versus emission angle θ_{lab} and in the intervals 2.5÷10.5 GeV/c($A_{2\pi}$) and 5÷14 GeV/c ($A_{\pi K}$) without taking into account the decays of pions and kaons in the setup. The relative yields of charged particles and atoms are W_{ch}^N=$W_{ch}/W_{ch}(5.7^\circ, 24\ GeV/c)$ and W_A^N=$W_A/W_A(5.7^\circ, 24\ GeV/c)$.

θ_{lab}	5.7°	4°	2°	0°
P_p	24 GeV/c	450 GeV/c	450 GeV/c	450 GeV/c
The yield of charged particles				
W_{ch}	0.022	0.14	0.50	2.9
W_{ch}^N	1	6.4	22.7	132
The yield of $\pi^+\pi^-$ atoms				
W_A	$1.94{\cdot}10^{-9}$	$3.4{\cdot}10^{-8}$	$6.9{\cdot}10^{-8}$	$8.9{\cdot}10^{-8}$
W_A^N	1	17.3	35.4	45.9
The yield of π^+K^- atoms				
W_A	$2.17{\cdot}10^{-10}$	$8.1{\cdot}10^{-9}$	$1.63{\cdot}10^{-8}$	$2.3{\cdot}10^{-8}$
W_A^N	1	37.5	75.	106.
The yield of $K^+\pi^-$ atoms				
W_A	$5.2{\cdot}10^{-10}$	$8.5{\cdot}10^{-9}$	$1.9{\cdot}10^{-8}$	$3.0{\cdot}10^{-8}$
W_A^N	1	16.4	37.6	57.4

flux of charged particles. Also this ratio is less sensitive to the accuracy of the meson production inclusive cross sections than the atomic absolute yield.

At $\theta_{lab} = 4^\circ$ and P_p=450 GeV/c where charged particle momenta are small and their identification is relatively simple the yields of $\pi^+\pi^-$, π^+K^- and $K^+\pi^-$ atoms are in 15, 67 and 31 times more respectively , than at $\theta_{lab} = 5.7^\circ$ and P_p=24 GeV/c. It means that it will be possible to decrease the proton beam intensity in several times to obtain the reduction of trigger events with accidental coincidences. The additional increasing of the atom production is connecting with beam time during supercycle on PS and SPS. At best condition the DIRAC had on PS the 4 spills with duration 0.45 s (full time 1.8 s). On SPS during the same supercycle the beam time is 4.6*2 = 9.6 s which gives the increasing for the atom production per time unit more than 5.

We can notice that at P_p=450 GeV/c the soft proton background is more than an order less than at 24 GeV/c [28, 25] decreasing on the order the background of $p\pi^-$ pairs to the $K^+\pi^-$ pairs.

4.3 Calculations of $R(\vec{p_1}, \vec{p_2}, S)$ at proton momentum 24 and 450 GeV/c for $\pi^+\pi^-$, π^+K^- and $K^+\pi^-$ pairs with small relative momentum.

The differential inclusive yield of atom production in (4) is expressed through double differential yield of two constituent particles. This yield we obtained using FTF generator. We can use the FTF to determine the correlation function (5) which allows to evaluate

Table 2: The yield of $\pi^+\pi^-$, π^+K^- and $K^+\pi^-$ atoms W_A into the aperture of 10^{-3} sr taking into account the setup acceptance and pion and kaon decays per one p-Ni interaction at the proton momenta P_p = 24 and 450 GeV/c versus emission angle θ_{lab}. W_A^N=$W_A/W_A(5.7^\circ, 24\ GeV/c)$ and $(W_A/W_ch)^N$=$(W_A/W_ch)/((W_A/W_ch)(5.7^\circ, 24\ GeV/c))$.

θ_{lab}	5.7°	4°	2°	0°
E_p	24 GeV/c	450 GeV/c	450 GeV/c	450 GeV
The yield of $\pi^+\pi^-$ atoms				
W_A	$1.25{\cdot}10^{-9}$	$1.9{\cdot}10^{-8}$	$3.5{\cdot}10^{-8}$	$4.5{\cdot}10^{-8}$
W_A^N	1	15	28	36
W_A/W_{ch}	$5.70{\cdot}10^{-8}$	$1.4{\cdot}10^{-7}$	$7.{\cdot}10^{-8}$	$1.6{\cdot}10^{-8}$
$(W_A/W_{ch})^N$	1	2.4	1.2	0.27
The yield of π^+K^- atoms				
W_A	$1.3{\cdot}10^{-11}$	$8.8{\cdot}10^{-10}$	$1.7{\cdot}10^{-9}$	$2.0{\cdot}10^{-9}$
W_A^N	1	67	131	154
W_A/W_{ch}	$5.9{\cdot}10^{-10}$	$6.3{\cdot}10^{-9}$	$3.4{\cdot}10^{-9}$	$6.9{\cdot}10^{-10}$
$(W_A/W_{ch})^N$	1	10.6	5.8	1.2
The yield of $K^+\pi^-$ atoms				
W_A	$3.1{\cdot}10^{-11}$	$9.7{\cdot}10^{-10}$	$2.1{\cdot}10^{-9}$	$2.7{\cdot}10^{-9}$
W_A^N	1	31	68	87
W_A/W_{ch}	$1.4{\cdot}10^{-9}$	$6.9{\cdot}10^{-9}$	$4.2{\cdot}10^{-9}$	$9.3{\cdot}10^{-10}$
$(W_A/W_{ch})^N$	1.	4.9	3.0	0.66

the value of W_A^N for all the dimesoatoms. Anyway it is important to know this correlation factor value and its dependence on particle pair momentum. This factor for the momentum interval of DIRAC setup is presented on Fig.20. It shows that the factor R for $\pi^+\pi^-$ pairs at P_p=24 GeV/c decreases from 1.25 (P_{pair} = 3 GeV/C) up to 0.5 (P_{pair} = 9 GeV/c). For $K\pi$ pairs R decreased from 1 (3 GeV/c) up to 0.5 (10 GeV/c). This decreasing is due to conservation low constrains. At P_p = 450 GeV/c the value of R practically does not depend on pair momentum and polar angle.

On Fig.20 we see that for all kinds of pairs the correlation function R at P_p = 24 GeV/c is less for all particle moments than the one at P_p = 450 GeV/c. The calculating of relative atom yields W_A^N with putting the correlation function R to 1 gives us the minimum value of W_A^N. In this case the error of W_A^N depends only on the uncertainties of inclusive cross section description by FTF which can be evaluate from experimental data analysis.

5 On the accuracy of FTF simulation results.

The production of atoms were calculated using (2) where the inclusive double cross section of pairs is used. It is impossible to get how well the FTF describes such value as there are no corresponding experimental data. In the equation (5) the double yield is presented via

the product of two single particle yields and a correlation factor R. It was shown(chapter 4.3) that if $R = 1$ then the minimum relative yield value is obtained. The precision of FTF description of single particle yield we can obtain from experimental distributions(Fig.1-9).

In the case of $A_{2\pi}$ atoms for $P_p = 24$ GeV/c we compared for MC and experimental data the product of π^+ and π^- distributions(Fig.2) in the pion momentum interval of 1÷3 GeV/c and for polar angle of 60÷100 $mrad$. The ratio of products $PR_{24\pi^+\pi^-} = PROD^{exp}_{24\pi^+\pi^-}/PROD^{MC}_{24\pi^+\pi^-} = 1.16\pm0.06$.

In the case of $A_{K^+\pi^-}$ atoms for $P_p = 24$ GeV/c we compared for MC and experimental data the product of K^+(Fig.6, 20÷140 $mrad$) and π^- distributions(Fig.2, 60÷100 $mrad$) in the kaon momentum interval of 4÷7 GeV/c. The ratio of products $PR_{24K^+\pi^-} = PROD^{exp}_{24K^+\pi^-}/PROD^{MC}_{24K^+\pi^-} = 0.78\pm0.06$.

In the case of $A_{K^-\pi^+}$ atoms for $P_p = 24$ GeV/c we compared for MC and experimental data the product of K^-(Fig.7, 100÷140 $mrad$) and π^+ distributions(Fig.2, 60÷100 $mrad$) in the kaon momentum interval of 4÷7 GeV/c. The ratio of products $PR_{24K^-\pi^+} = PROD^{exp}_{24K^-\pi^+}/PROD^{MC}_{24K^-\pi^+} = 0.90\pm0.07$.

For $P_p = 450$ GeV/c case the possibility in comparing of product of pion and kaon distributions is very poor. Here we can use the only point in experimental invariant inclusive cross sections of π^+, π^-, K^+ and K^- in p-Be interactions at 450 GeV/c as function of particle momentum in the forward direction(Fig.9). This point corresponds to $P_{\pi^+,\pi^-,K^+,K^-} = 7$ GeV/c.

The same ratios for $P_p = 450$ GeV/c($PR_{450\pi^+\pi^-}$,$PR_{450K^+\pi^-}$ and $PR_{450K^-\pi^+}$) are equal 0.87±0.13, 0.75±0.12 and 0.82±0.17 correspondingly.

These correction factors we used to estimate the minimal gain of atom production at $P_p = 450$ GeV/c with comparison with $P_p = 24$ GeV/c (Tab.3,4).

Table 3: The yield $W_A(R=1)$ of $\pi^+\pi^-$, π^+K^- and $K^+\pi^-$ atoms with $R=1$ into the aperture of 10^{-3} sr taking into account the setup acceptance and pion and kaon decays per one p-Ni interaction at the proton momenta $P_p = 24$ and 450 GeV/c versus emission angle θ_{lab}. The ratio $(W_A(R=1))^N = W_A(R=1,\ 450GeV/c)/W_A(R=1,\ 5.7^\circ, 24GeV/c)$ gives the minimum value of ratio of atom yields at $P_p = 450$ GeV/c and $P_p = 24$ GeV/c.

θ_{lab}	5.7°	4°	2°	0°
E_p	24 GeV/c	450 GeV/c	450 GeV/c	450 GeV
The yield of $\pi^+\pi^-$ atoms				
$W_A(R=1)$	$(1.73 \pm 0.09) \cdot 10^{-9}$	$(1.7 \pm 0.2) \cdot 10^{-8}$	$(3.0 \pm 0.5) \cdot 10^{-8}$	$(3.9 \pm 0.6) \cdot 10^{-8}$
$(W_A(R=1))^N$	1	9.7 ± 1.5	17.5 ± 2.8	22.7 ± 3.6
The yield of π^+K^- atoms				
$W_A(R=1)$	$(1.46 \pm 0.09) \cdot 10^{-11}$	$(6.6 \pm 1.1) \cdot 10^{-10}$	$(1.31 \pm 0.21) \cdot 10^{-9}$	$(1.52 \pm 0.24) \cdot 10^{-9}$
$(W_A(R=1))^N$	1	45 ± 8	87 ± 15	104 ± 18
The yield of $K^+\pi^-$ atoms				
$W_A(R=1)$	$(4.2 \pm 0.3) \cdot 10^{-11}$	$(7.9 \pm 1.6) \cdot 10^{-10}$	$(1.8 \pm 0.4) \cdot 10^{-9}$	$(2.2 \pm 0.5) \cdot 10^{-9}$
$(W_A(R=1))^N$	1	18.6 ± 4.1	41 ± 9	52 ± 11

Table 4: The relative yields $W_A(R=1)/W_{ch}$ of $\pi^+\pi^-$, π^+K^- and $K^+\pi^-$ atoms into the aperture of 10^{-3} sr taking into account the setup acceptance and pion and kaon decays per one p-Ni interaction at the proton momenta $P_p = 24$ and 450 GeV/c versus emission angle θ_{lab}. $(W_A(R=1)/W_{ch})^N$=$(W_A(R=1)/W_{ch})/((W_A(R=1)/W_{ch})(5.7^\circ, 24\ GeV/c))$.

θ_{lab}	5.7°	4°	2°	0°
E_p	24 GeV/c	450 GeV/c	450 GeV/c	450 GeV
The yield of $\pi^+\pi^-$ atoms				
$W_A(R=1)/W_{ch}$	$7.8 \pm 0.4) \cdot 10^{-8}$	$(1.21 \pm 0.14) \cdot 10^{-7}$	$(6.0 \pm 1.0) \cdot 10^{-8}$	$(1.34 \pm 0.21) \cdot 10^{-8}$
$(W_A(R=1)/W_{ch})^N$	1	1.55 ± 0.20	$0.77 \pm /13$	$.17 \pm 0.03$
The yield of π^+K^- atoms				
$W_A(R=1)/W_{ch}$	$(6.6 \pm 0.4) \cdot 10^{-10}$	$(4.7 \pm 0.8) \cdot 10^{-9}$	$(2.6 \pm 0.4) \cdot 10^{-9}$	$(5.2 \pm 0.8) \cdot 10^{-10}$
$(W_A(R=1)/W_{ch})^N$	1	$7. \pm 1.$	3.9 ± 0.7	0.79 ± 0.13
The yield of $K^+\pi^-$ atoms				
$W_A(R=1)/W_{ch}$	$(1.91 \pm 0.14) \cdot 10^{-9}$	$(5.6 \pm 1.1) \cdot 10^{-9}$	$(3.6 \pm 0.8) \cdot 10^{-9}$	$(7.6 \pm 1.7) \cdot 10^{-10}$
$(W_A(R=1)/W_{ch})^N$	1	2.9 ± 0.6	1.9 ± 0.4	0.40 ± 0.09

6 Conclusion.

1. The performed analysis shows that the atom production in the p-nucleus interactions is increasing more than the order of magnitude if the momentum of proton P_p will change from 24 up to 450 GeV/c.

2. At $\theta_{lab} = 0^\circ$ and P_p=450 GeV/c the yields of $\pi^+\pi^-$, π^+K^- and $K^+\pi^-$ atoms are in 46, 106 and 57 times more respectively , than at $\theta_{lab} = 5.7^\circ$ and P_p=24 GeV/c in the same solid angle.

3. If we take into account the acceptance of setup like DIRAC (PS212) then at $\theta_{lab} = 4^\circ$ and P_p=450 GeV/c the yields of $\pi^+\pi^-$, π^+K^- and $K^+\pi^-$ atoms are in 15, 67 and 31 times more respectively , than at $\theta_{lab} = 5.7^\circ$ and P_p=24 GeV/c .

4. Practically the model independent estimation of these minimum value yields gives that the yields of $\pi^+\pi^-$, π^+K^- and $K^+\pi^-$ atoms at $\theta_{lab} = 4^\circ$ and P_p=450 GeV/c are at least in 10, 45 and 19 times more respectively , than at $\theta_{lab} = 5.7^\circ$ and P_p=24 GeV/c .

5. Taking in to account the duty factor of PS and SPS the previous yields in the time unity will be increased to 4 times more.

6. The large yield of dimesoatoms at P_p=450 GeV/c allows to use the primary proton beam with lower intensity and decrease the trigger events connecting with accidentals.

7 Acknowledgements

We are grateful to M.Gadzitski and A.Korzenev for offering of unpublished data on inclusive cross sections for p-C interactions at P_p = 31 GeV/c. We are grateful also to V.Uzhinsky for the consulting on FTF generator.

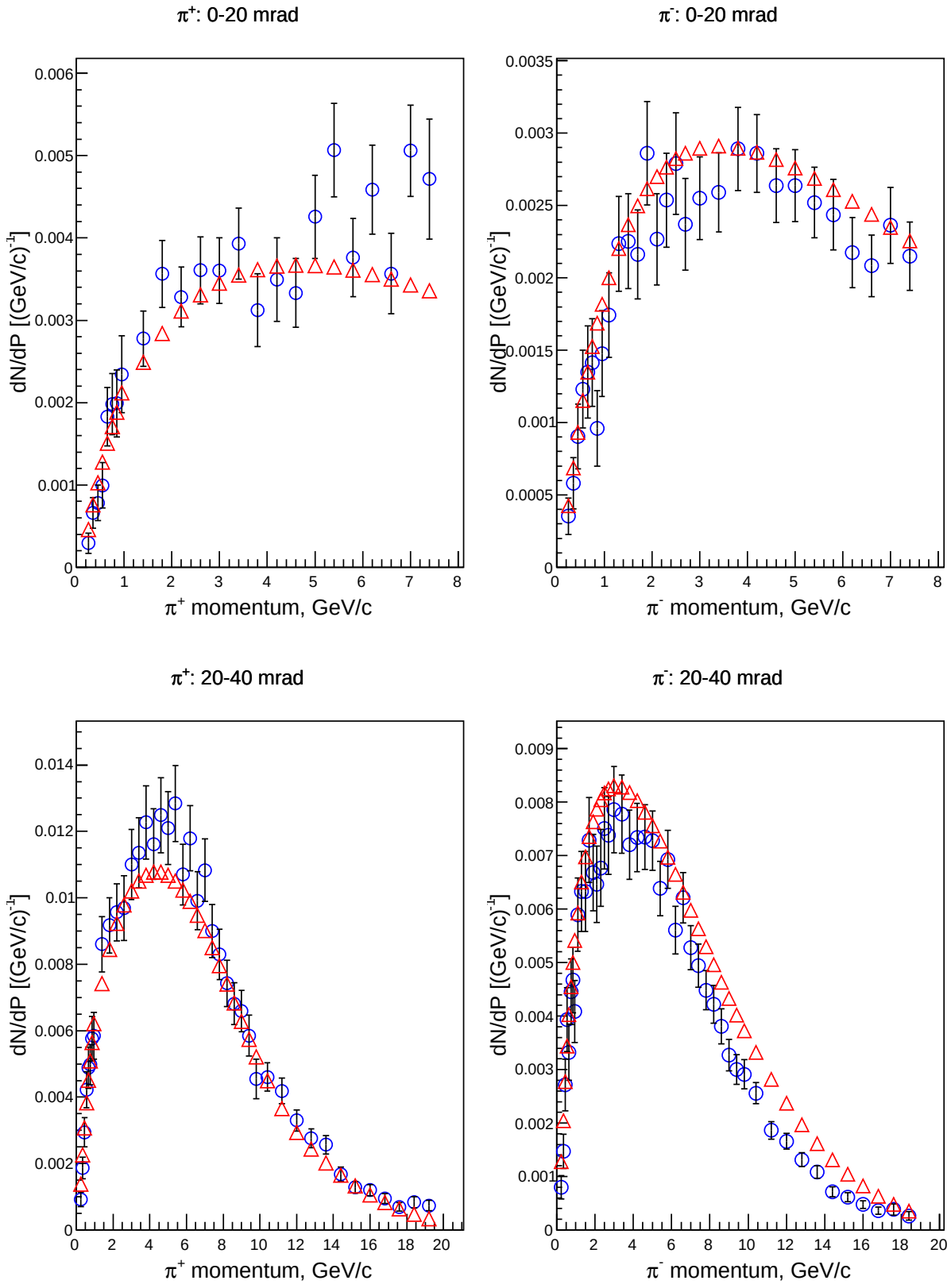

Figure 1: The yields of π^+ and π^- in p-C interactions at 31 GeV/c for polar angles 0÷20 and 20÷40 *mrad*. ○ - experimental data [24] and △ - FTF simulation data.

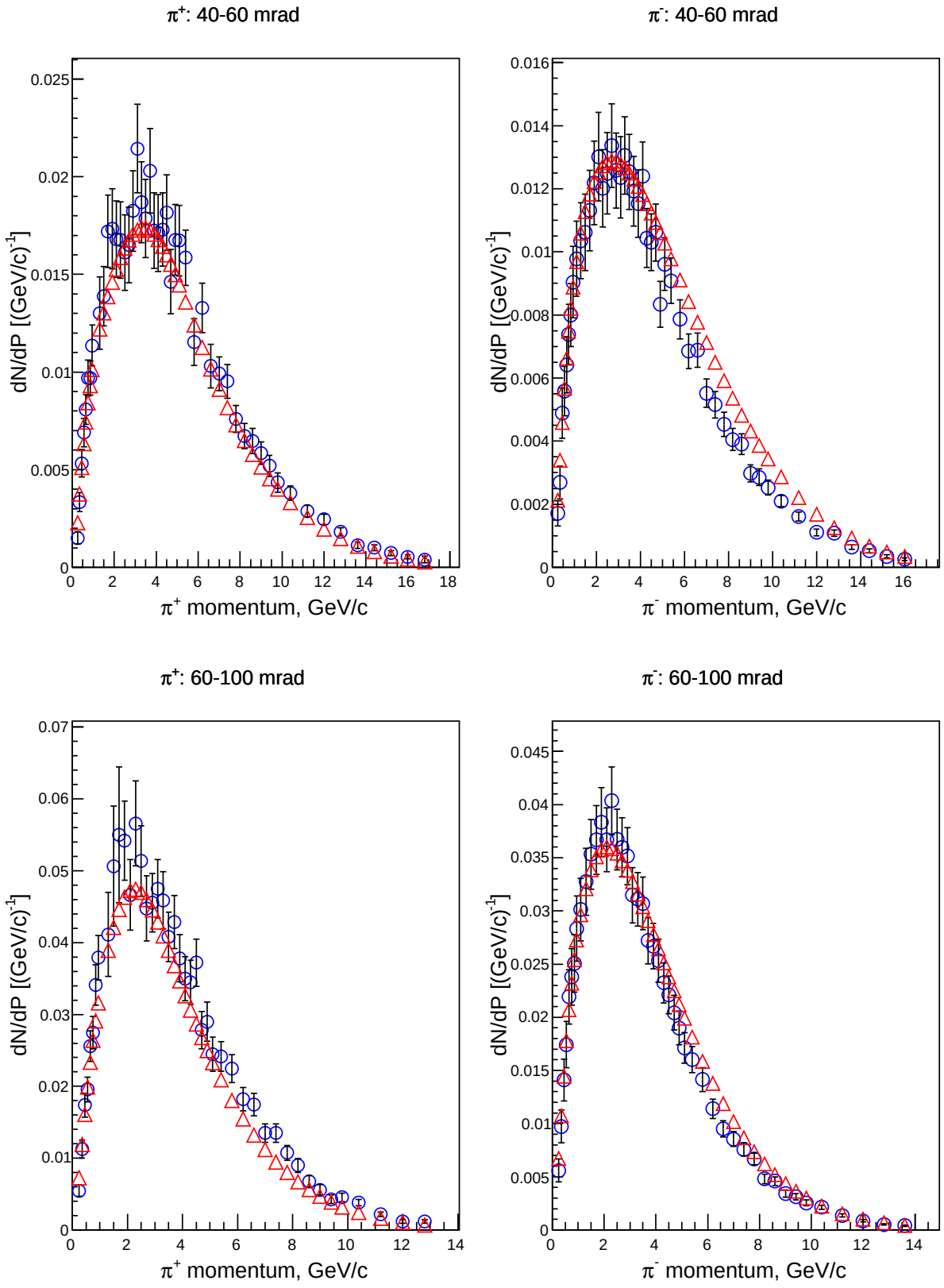

Figure 2: The yields of π^+ and π^- in p-C interactions at 31 GeV/c for polar angles 40÷60 and 60÷100 *mrad*. ○ - experimental data [24] and △ - FTF simulation data.

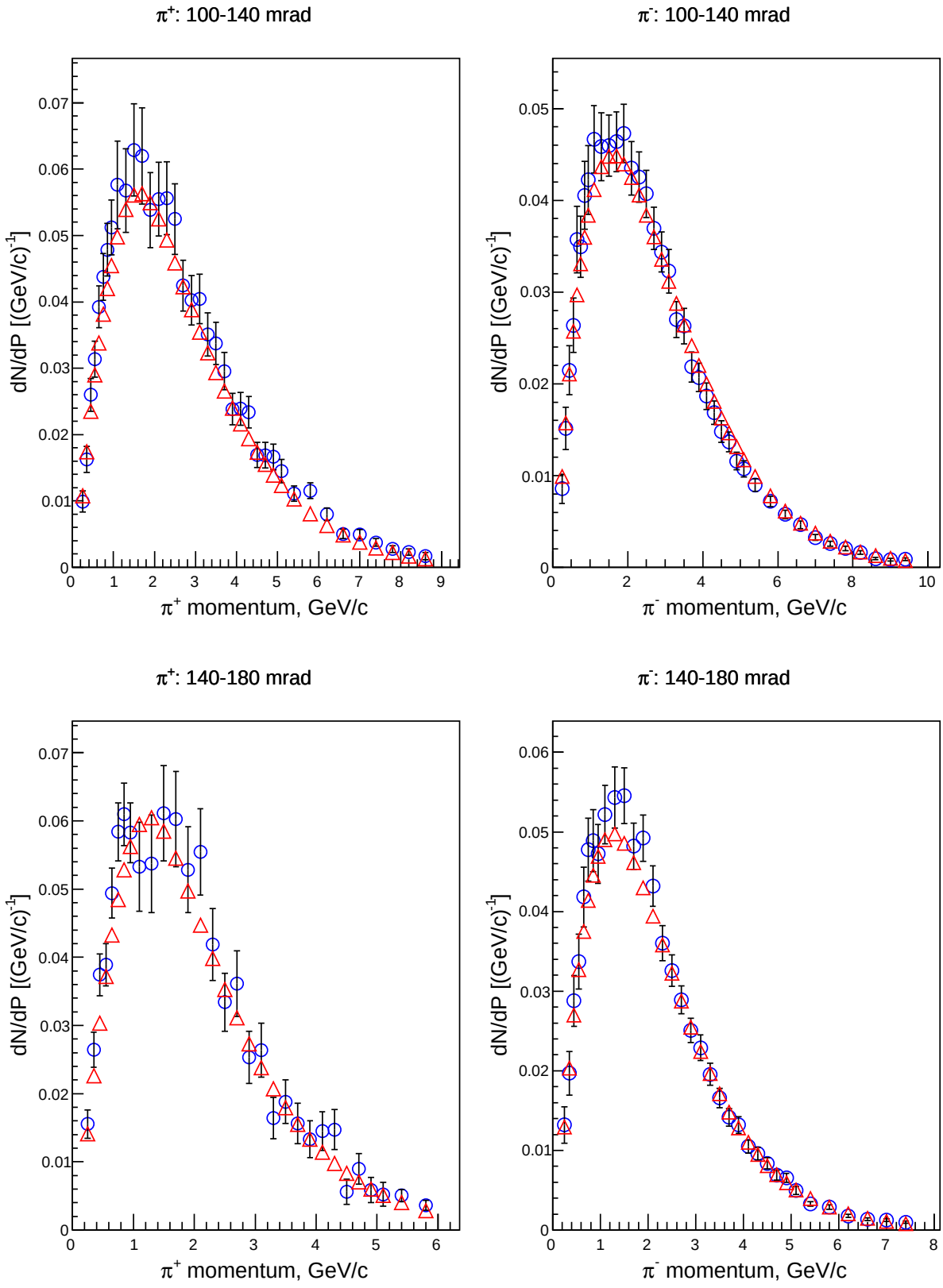

Figure 3: The yields of π^+ and π^- in p-C interactions at 31 GeV/c for polar angles 100÷140 and 140÷180 *mrad*. ○ - experimental data [24] and △ - FTF simulation data.

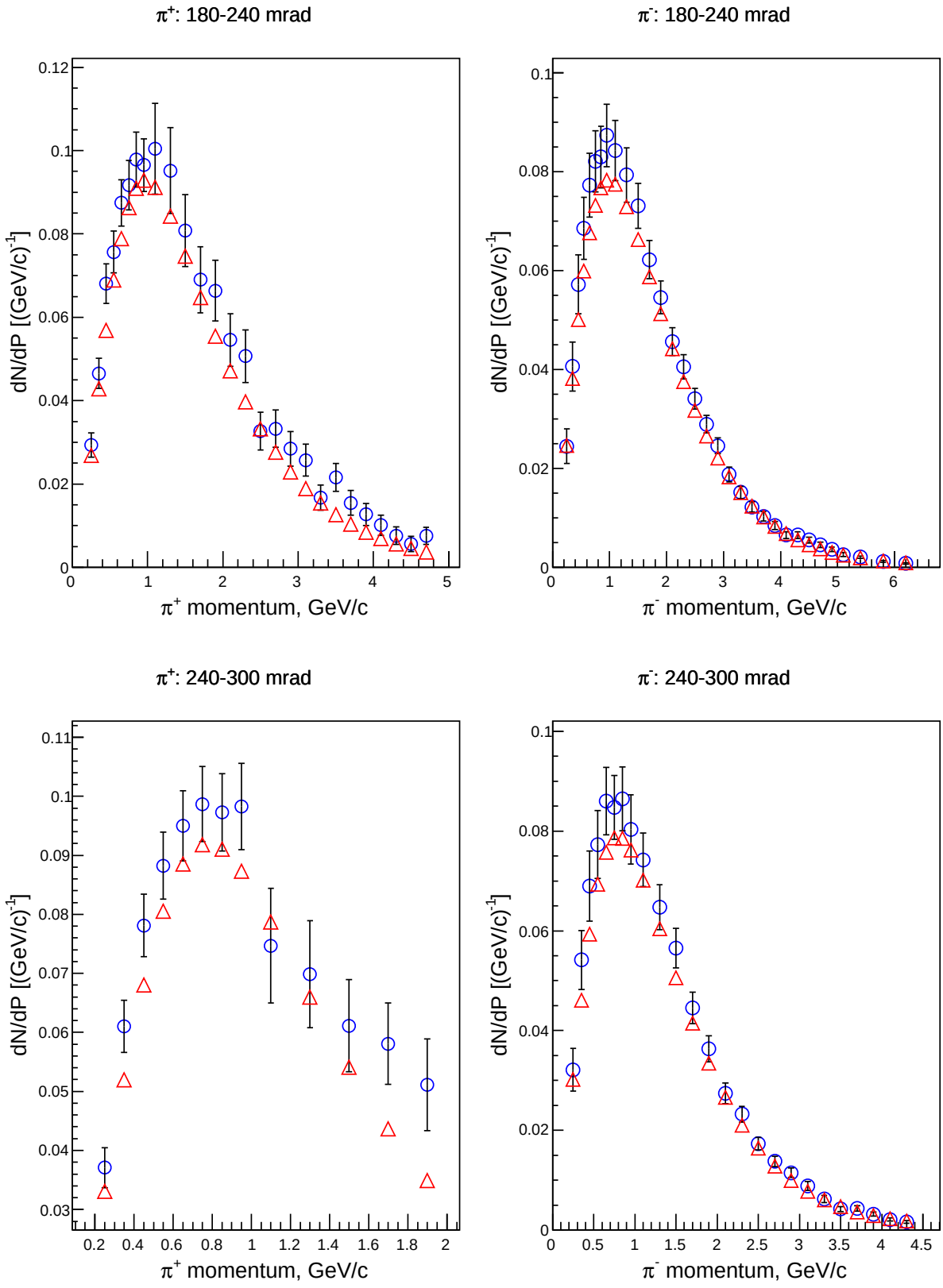

Figure 4: The yields of π^+ and π^- in p-C interactions at 31 GeV/c for polar angles 180÷240 and 240÷300 *mrad*. ○ - experimental data [24] and △ - FTF simulation data.

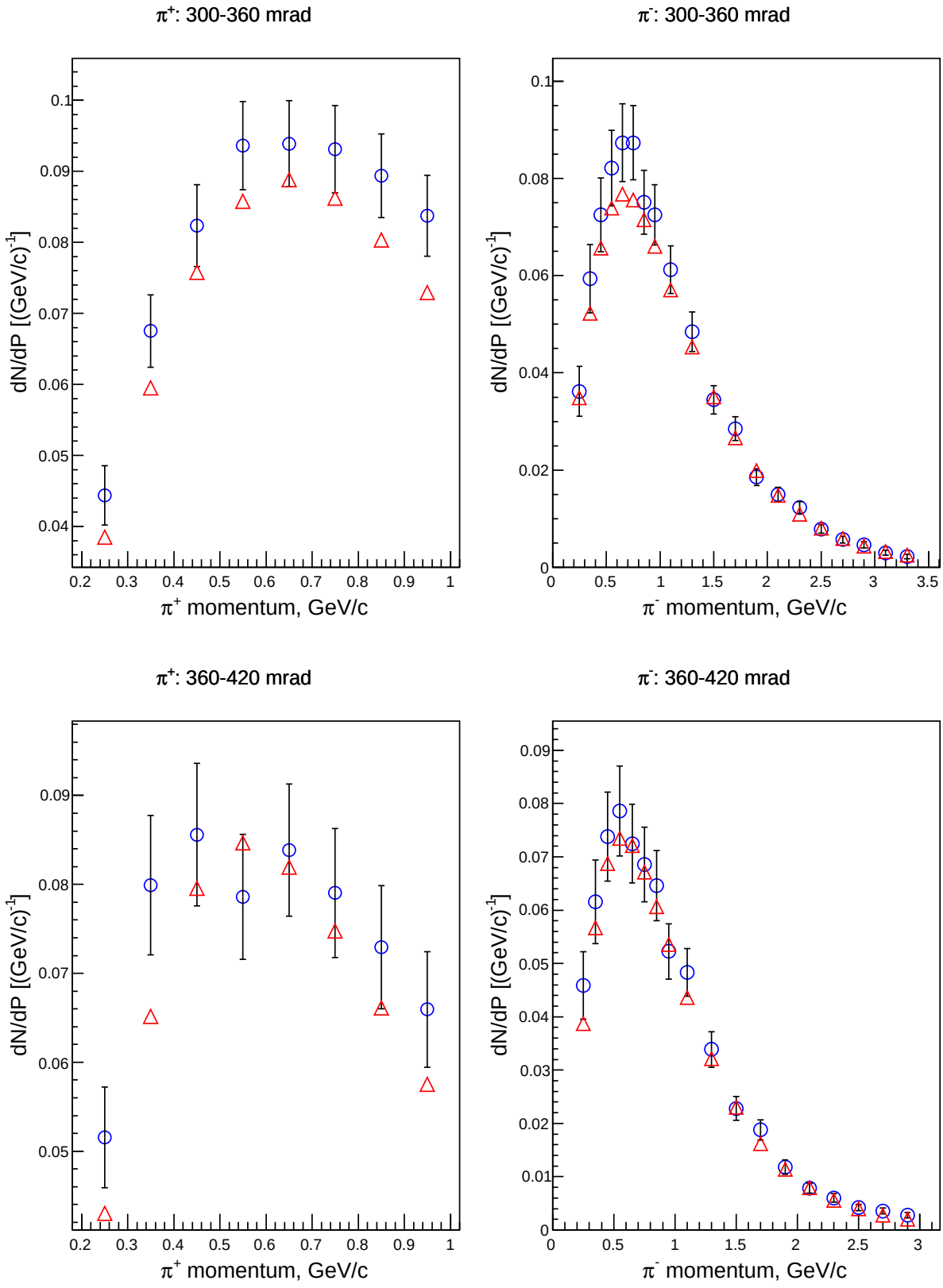

Figure 5: The yields of π^+ and π^- in p-C interactions at 31 GeV/c for polar angles 300÷360 and 360÷420 *mrad*. ○ - experimental data [24] and △ - FTF simulation data.

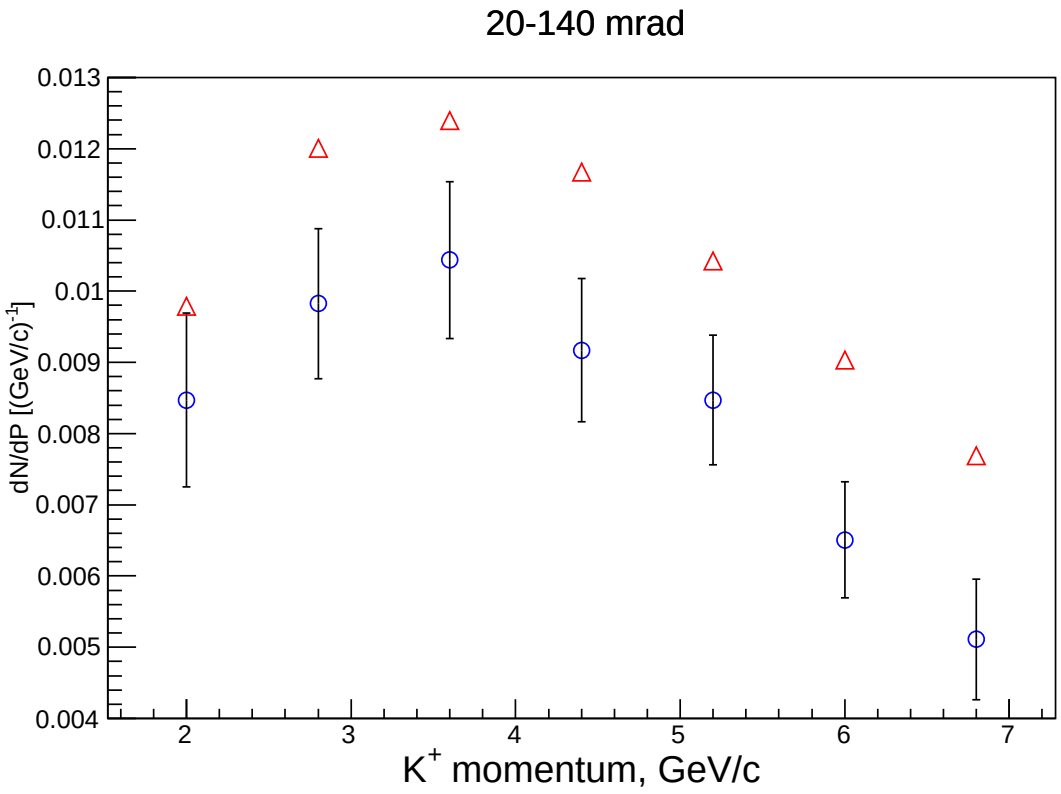

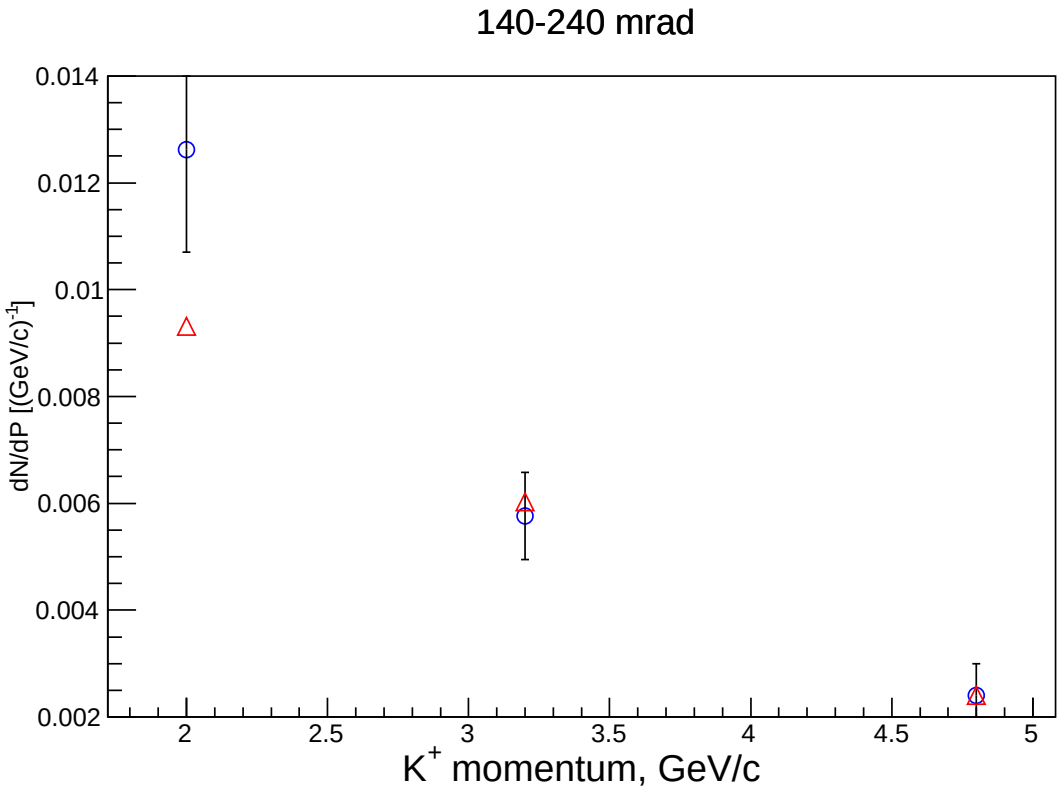

Figure 6: The yields of K^+ in p-C interactions at 31 GeV/c for polar angles 20÷140 and 140÷240 *mrad*. ○ - experimental data [24] and △ - FTF simulation data.

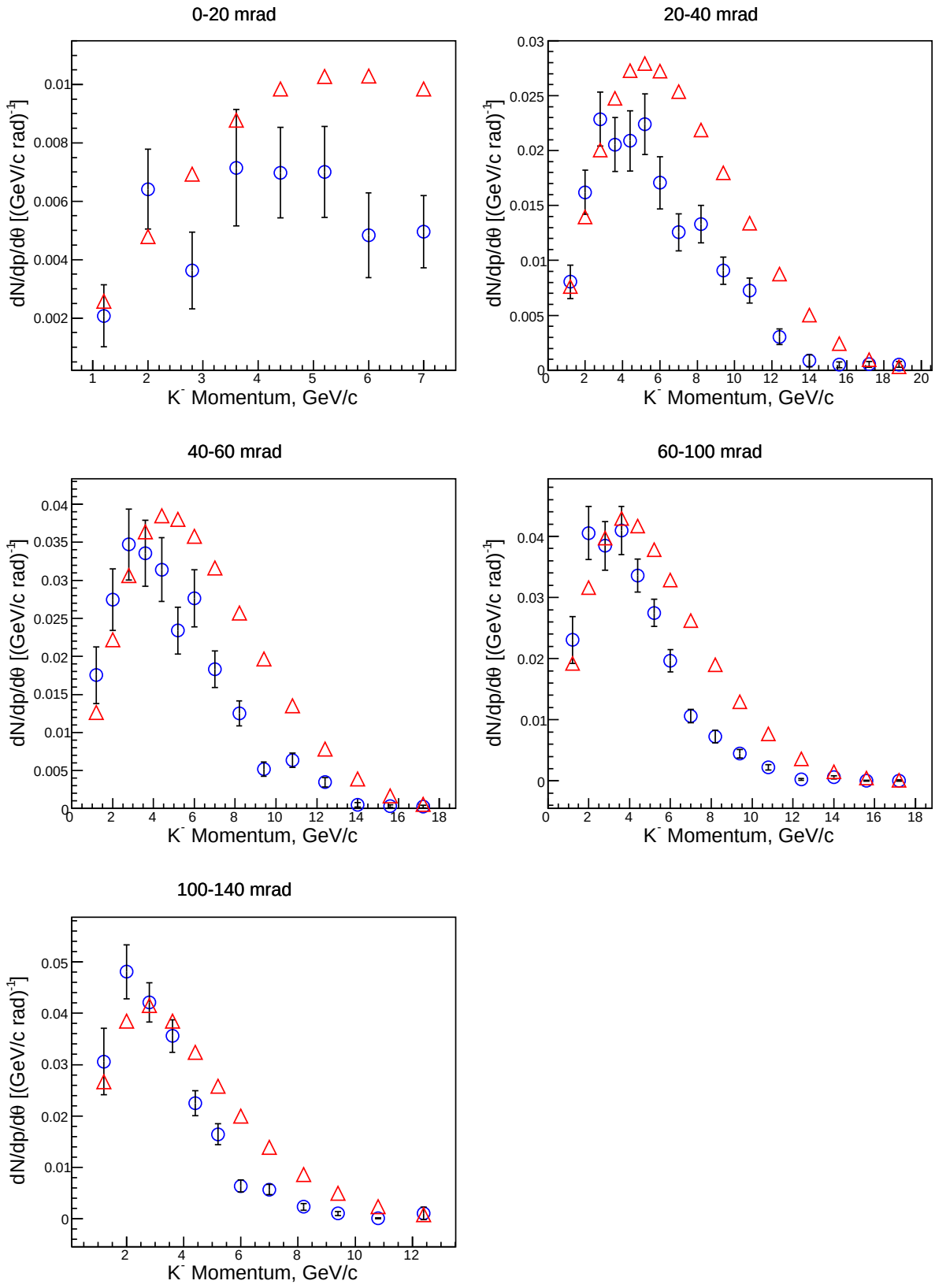

Figure 7: The yields of K^- in p-C interactions at 31 GeV/c for polar angles θ_{lab} 0÷20,20÷40,40÷60, 60÷100 and 100÷140 *mrad*. ○ - experimental data [24] and △ - FTF simulation data.

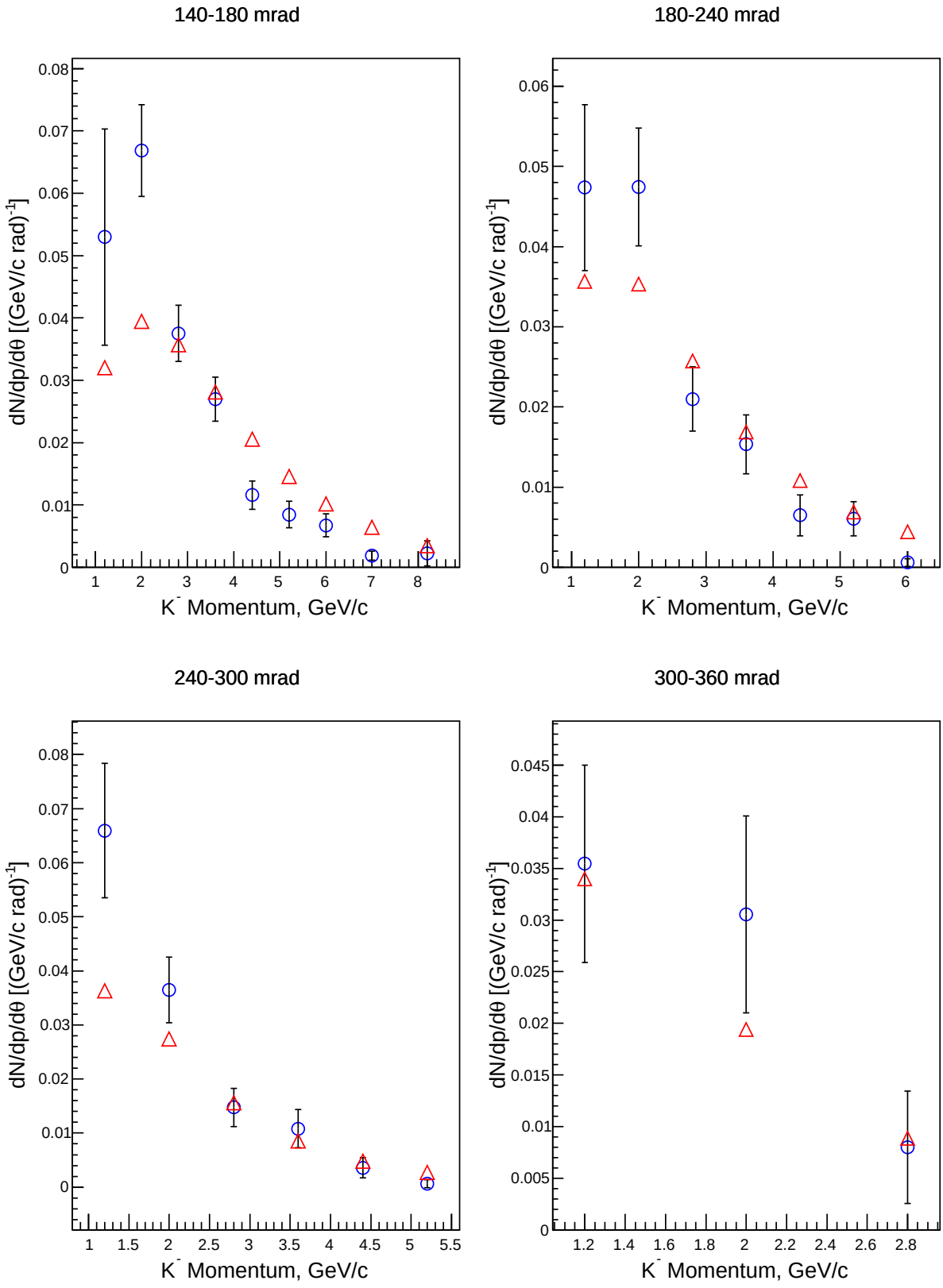

Figure 8: The yields of K^- in p-C interactions at 31 GeV/c for polar angles θ_{lab} 140÷180,180÷240,240÷300 and 3000÷360 *mrad*. ○ - experimental data [24] and △ - FTF simulation data.

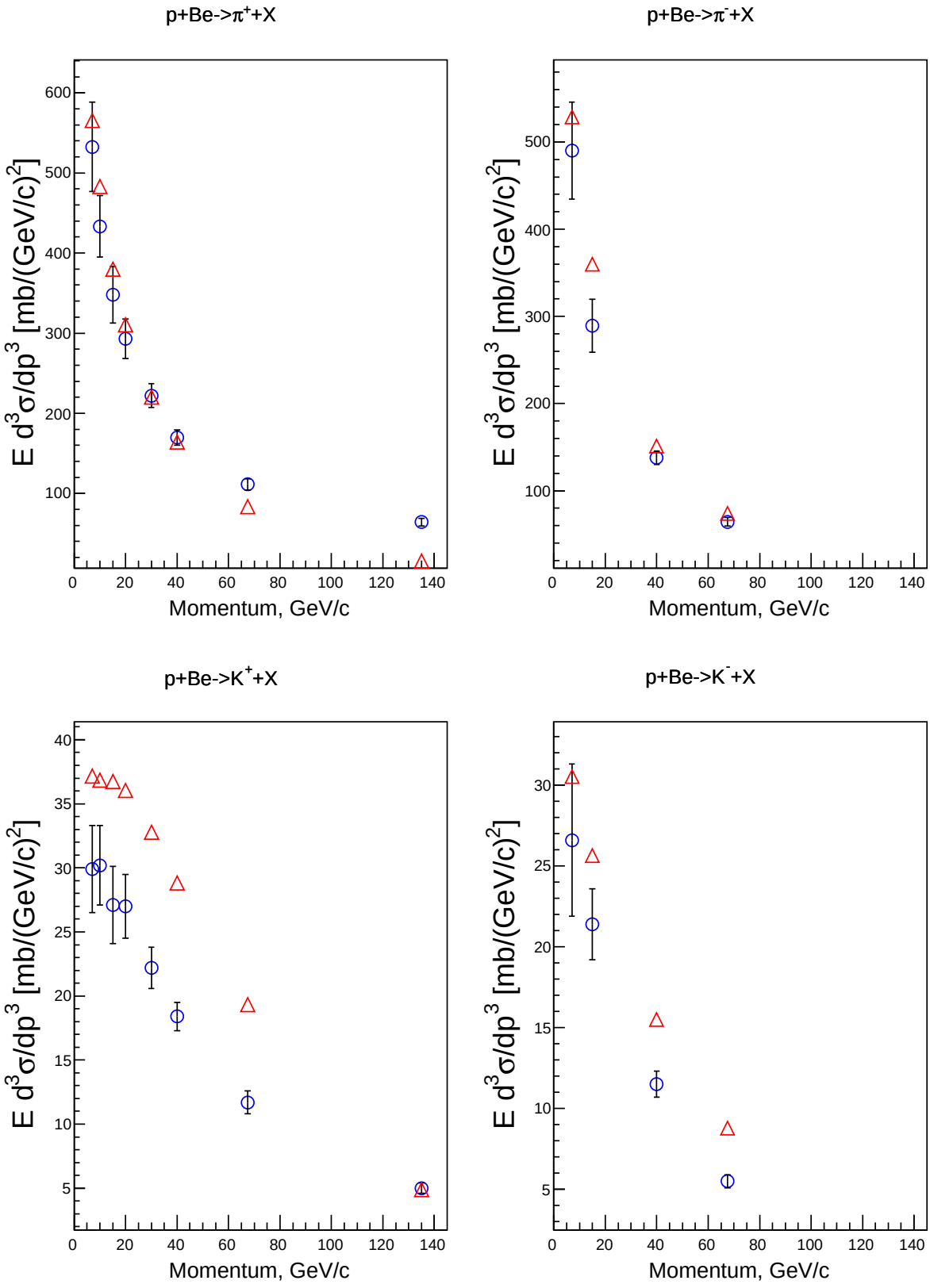

Figure 9: The invariant inclusive cross sections of π^+, π^-, K^+ and K^- in p-Be interactions at 450 GeV/c as function of particle momentum in the forward direction. ○ - experimental data [24] and △ - FTF simulation data.

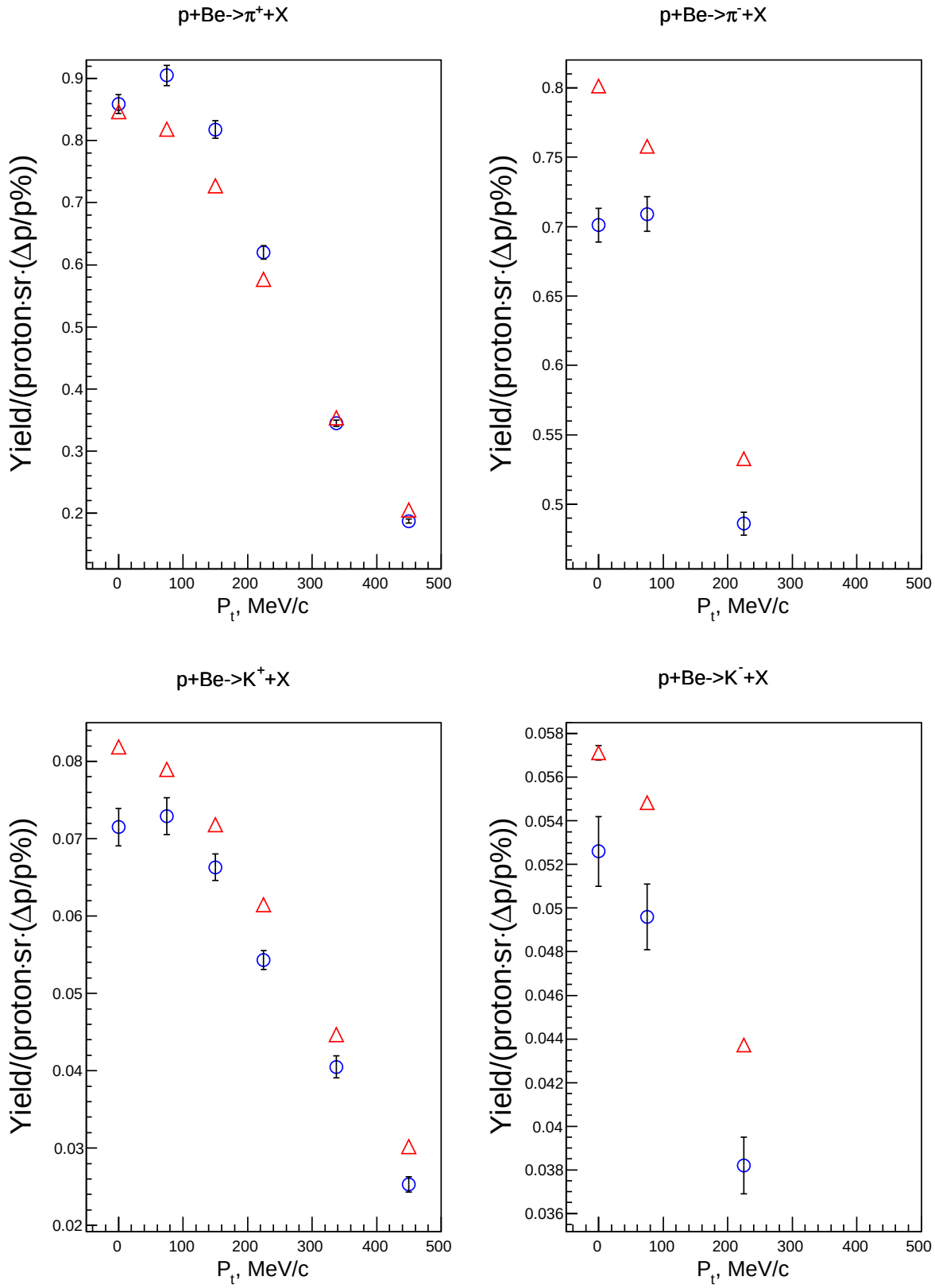

Figure 10: The yields of π^+, π^-, K^+ and K^- in p-Be interactions at 450 GeV/c as function of P_t. ○ - experimental data [24] and △ - FTF simulation data.

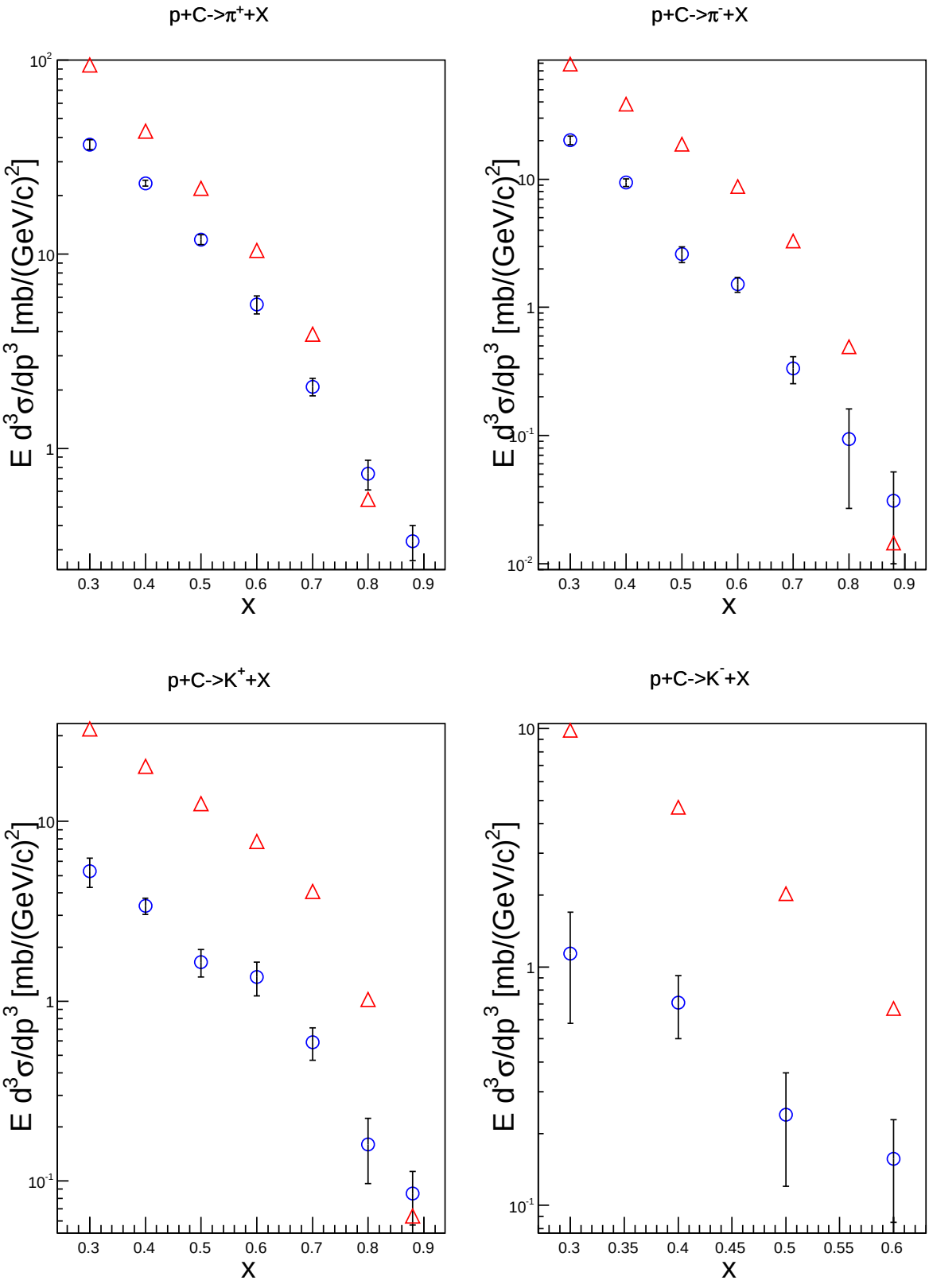

Figure 11: The yields of π^+, π^-, K^+ and K^- in p-C interactions for $P_t = 0.3$ GeV/c as function of x at 100 GeV/c. ○ - experimental data [24] and △ - FTF simulation data.

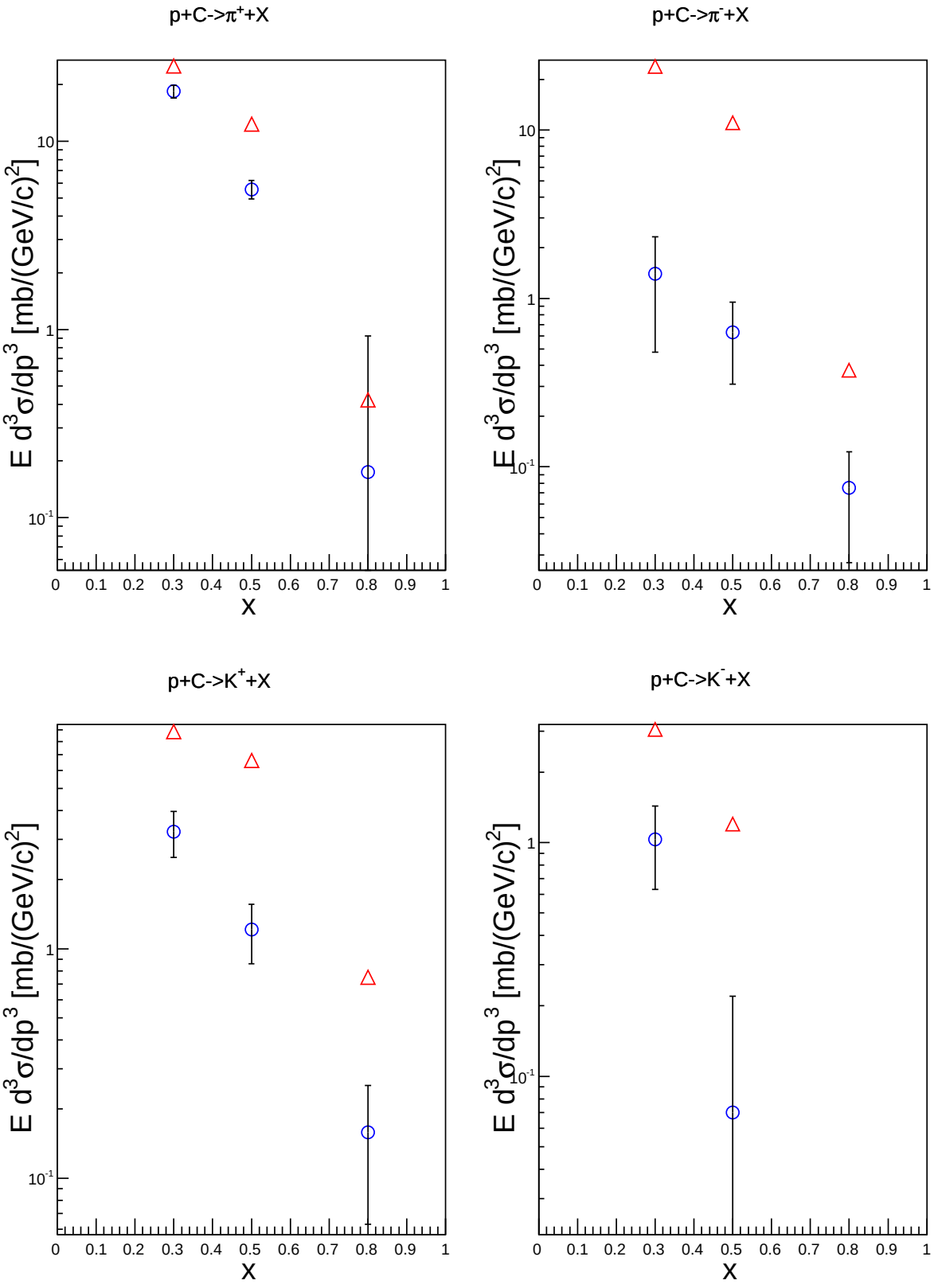

Figure 12: The yields of π^+, π^-, K^+ and K^- in p-C interactions for $P_t = 0.5\ GeV/c$ as function of x at 100 GeV/c. ○ - experimental data [24] and △ - FTF simulation data.

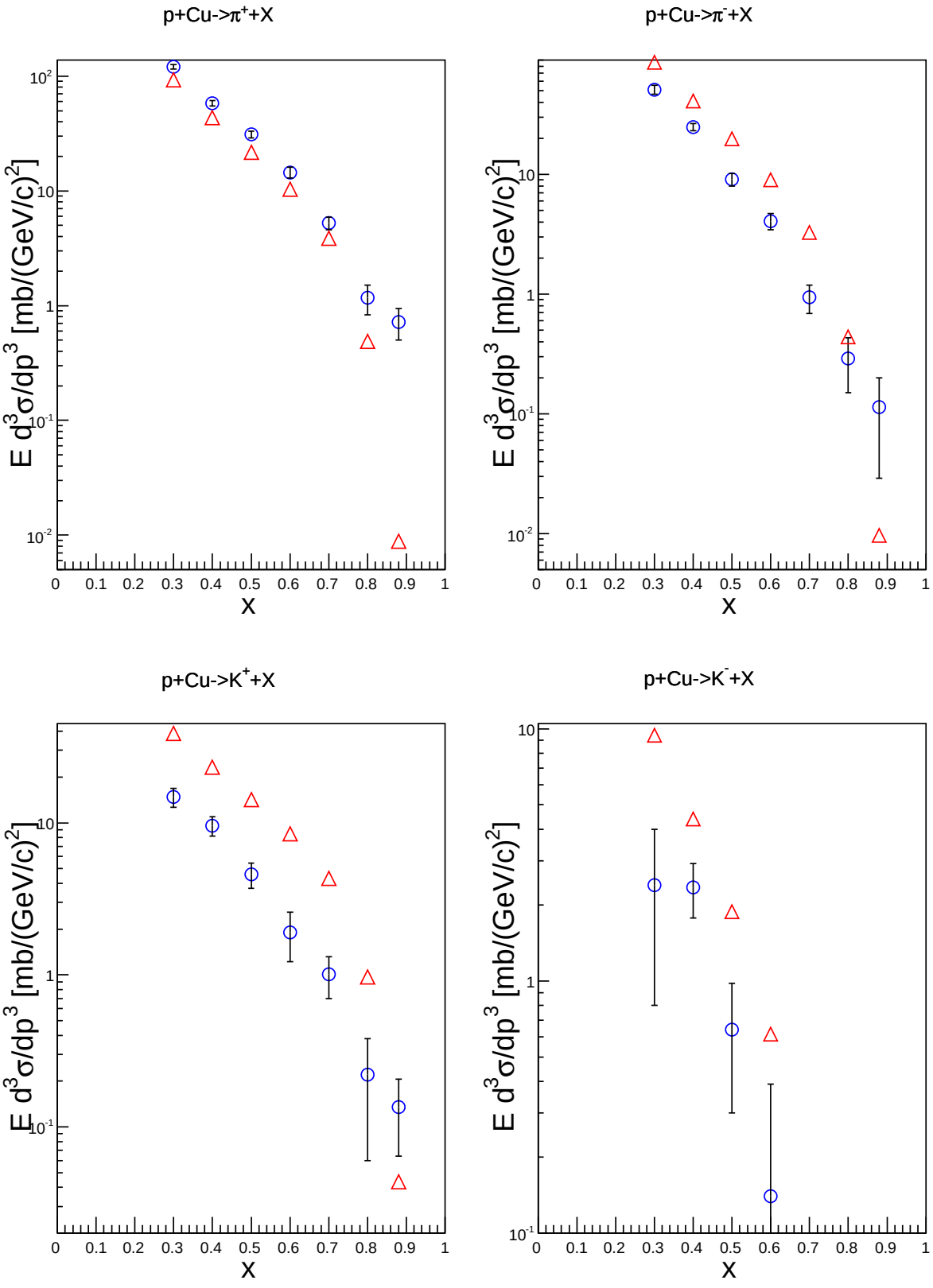

Figure 13: The yields of π^+, π^-, K^+ and K^- in p-Cu interactions for $P_t = 0.3\ GeV/c$ as function of x at 100 GeV/c. ○ - experimental data [24] and △ - FTF simulation data.

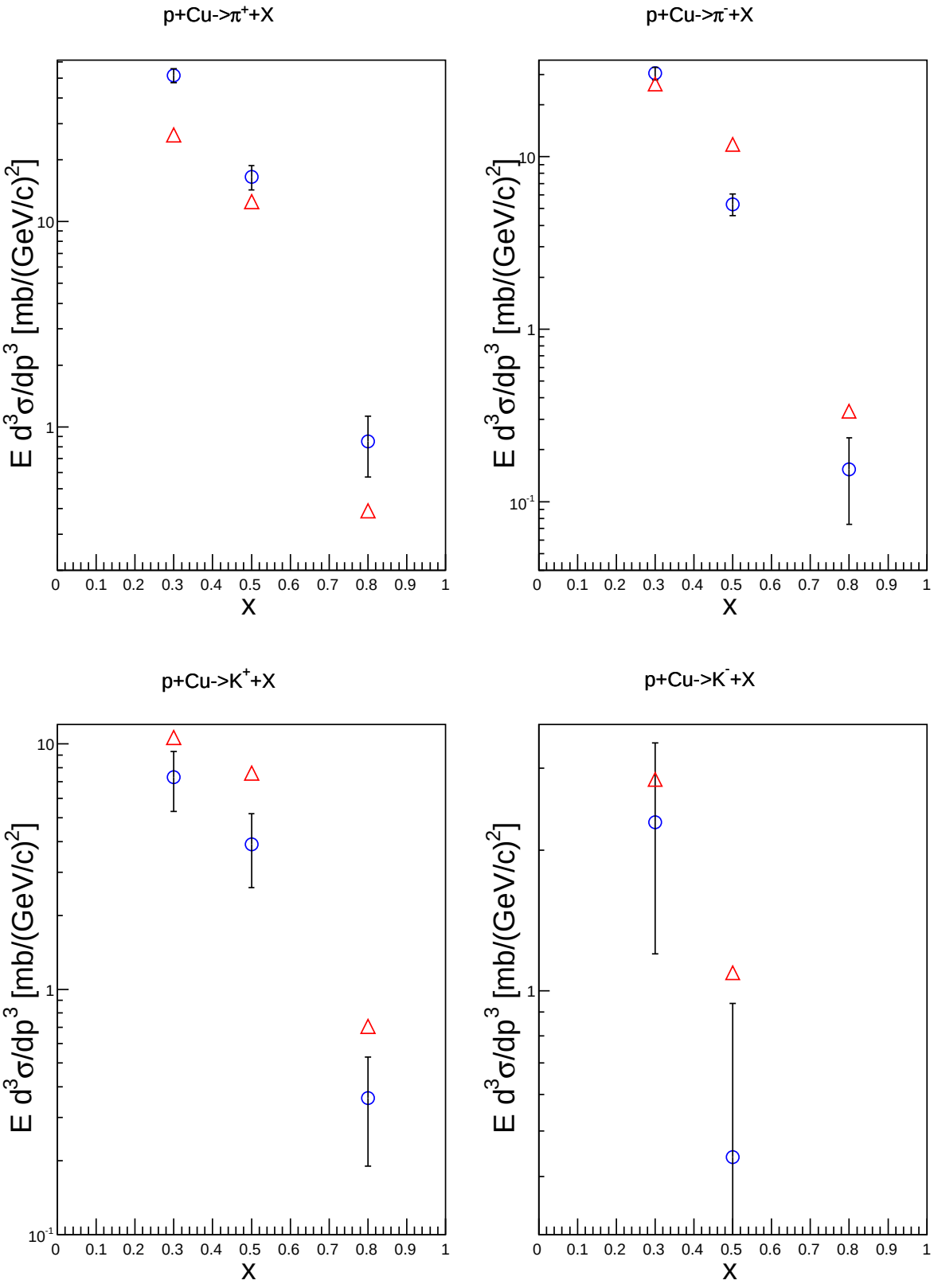

Figure 14: The yields of π^+, π^-, K^+ and K^- in p-Cu interactions for $P_t = 0.5\ GeV/c$ as function of x at 100 GeV/c. ○ - experimental data [24] and △ - FTF simulation data.

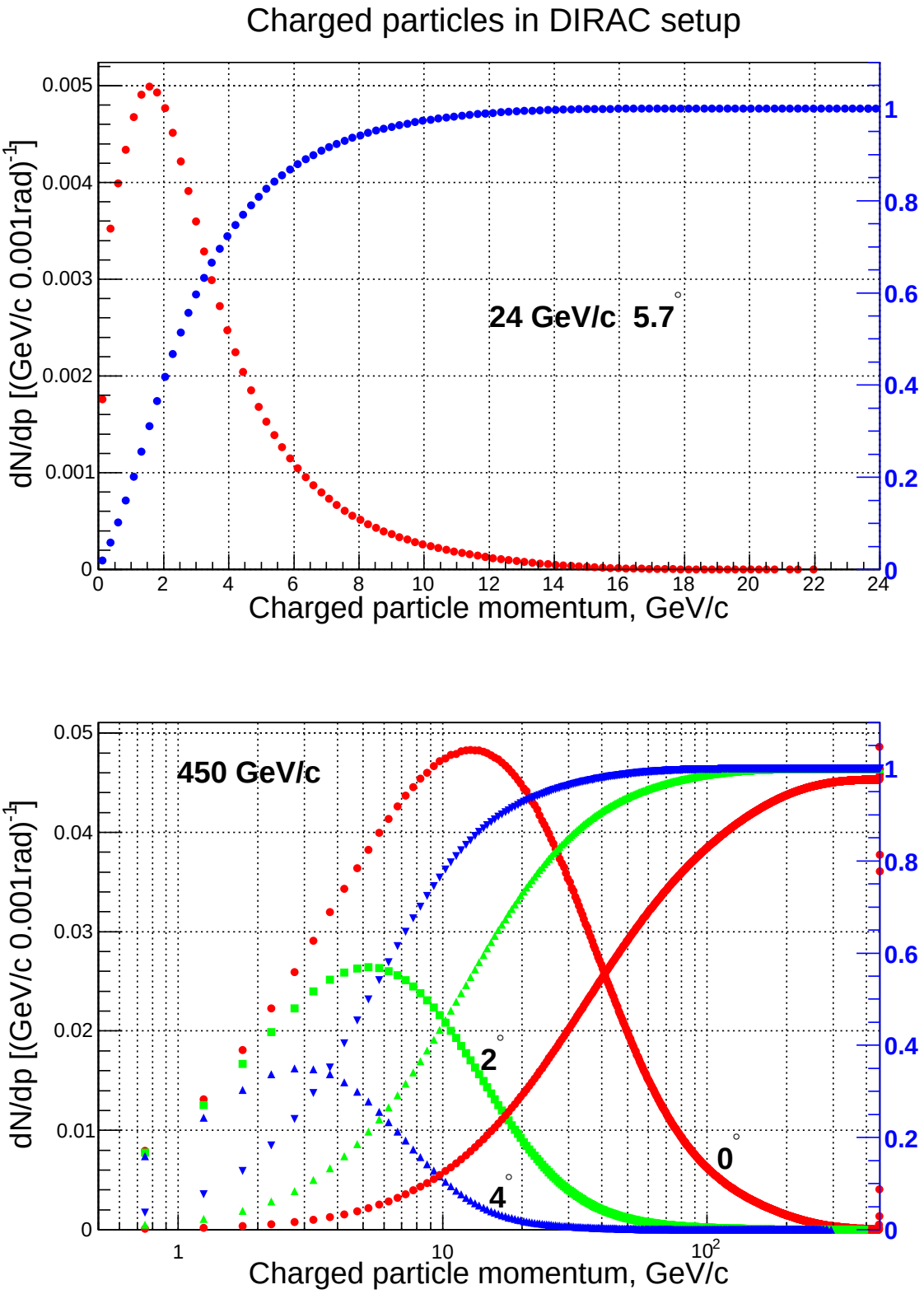

Figure 15: The total yield of charged particles ($\pi^{\pm}$, $K^{\pm}$, p and $\bar{p}$) per one p-Ni interaction at the proton momentum 450 GeV/c and emission angles $\theta_{lab} = 0°$, $2°$, $4°$(bottom) and at the proton momentum 24 GeV/c and emission angle $\theta_{lab} = 5.7°$(top) as a function of their momentum in l.s. for solid angle of 10^{-3} sr. Also the integrated and normalized to 1 distributions are shown.

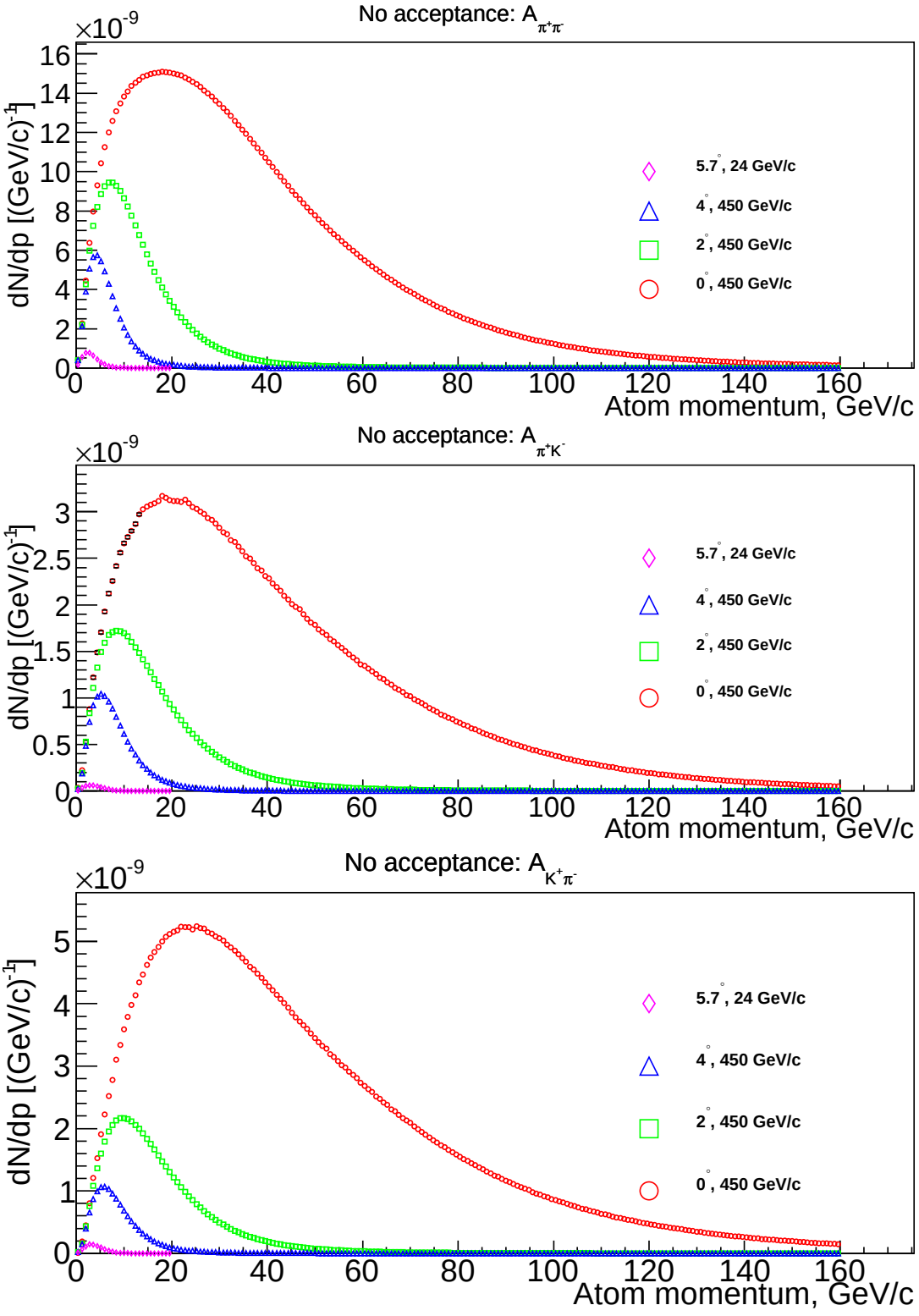

Figure 16: Yields of $A_{2\pi}$, $A_{\pi K}$ and $A_{K\pi}$ atoms per one p-Ni interaction at the proton momentum 450 GeV/c and emission angles $\theta_{lab} = 0°$, $2°$, $4°$ and at the proton momentum 24 GeV/c and emission angle $\theta_{lab} = 5.7°$ as a function of the atom momentum in l.s for solid angle of 10^{-3} sr. The acceptance is not taken into account.

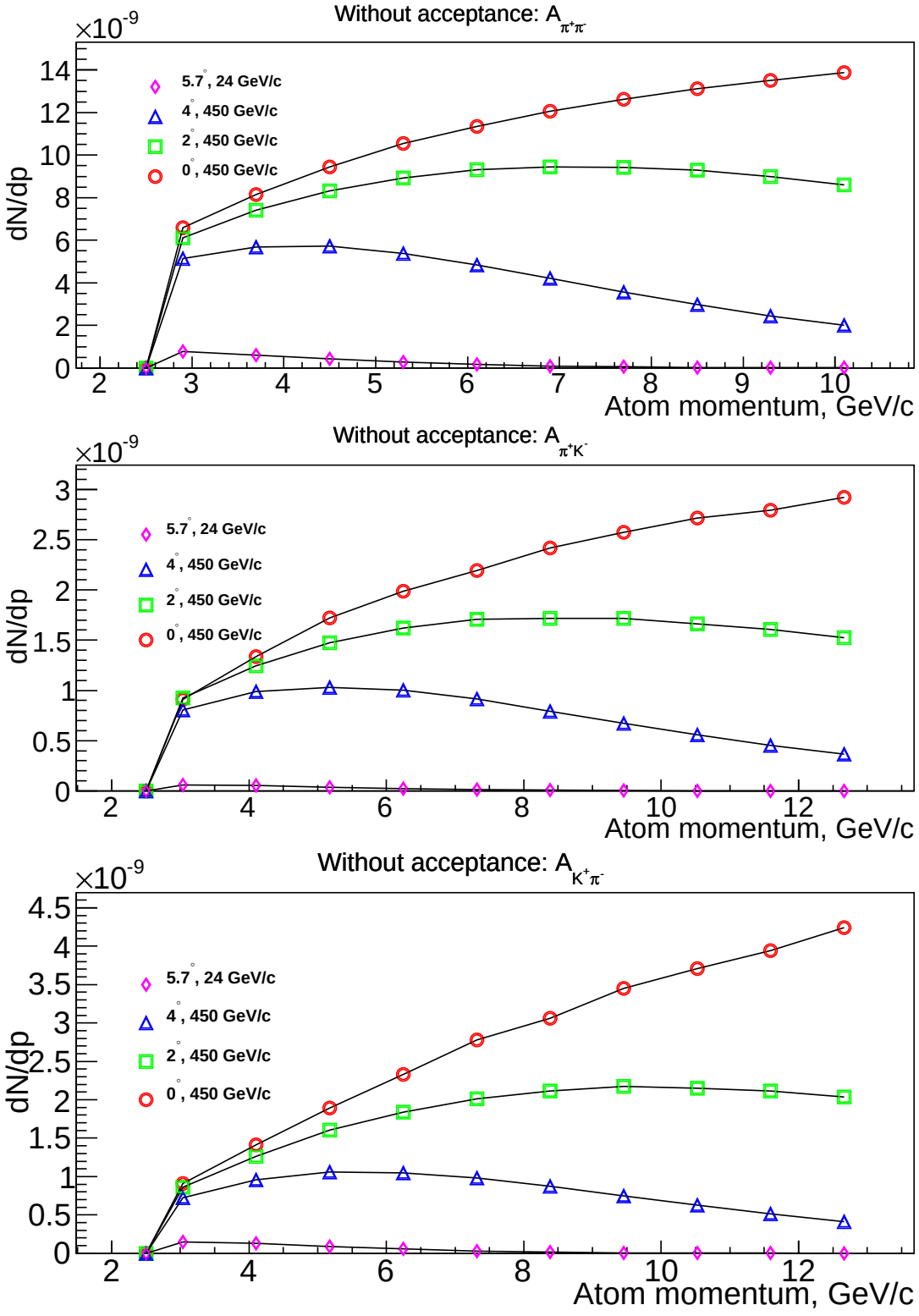

Figure 17: Yields of $A_{2\pi}$, $A_{\pi K}$ and $A_{K\pi}$ atoms per one p-Ni interaction in solid angle 10^{-3} sr at the proton momentum 450 GeV/c and emission angles $\theta_{lab} = 0°$, $2°$, $4°$ and at the proton momentum 24 GeV/c and emission angle $\theta_{lab} = 5.7°$ as a function of the atom momentum in l.s. and in the momentum interval which corresponds to DIRAC setup. The decays are not taken into account.

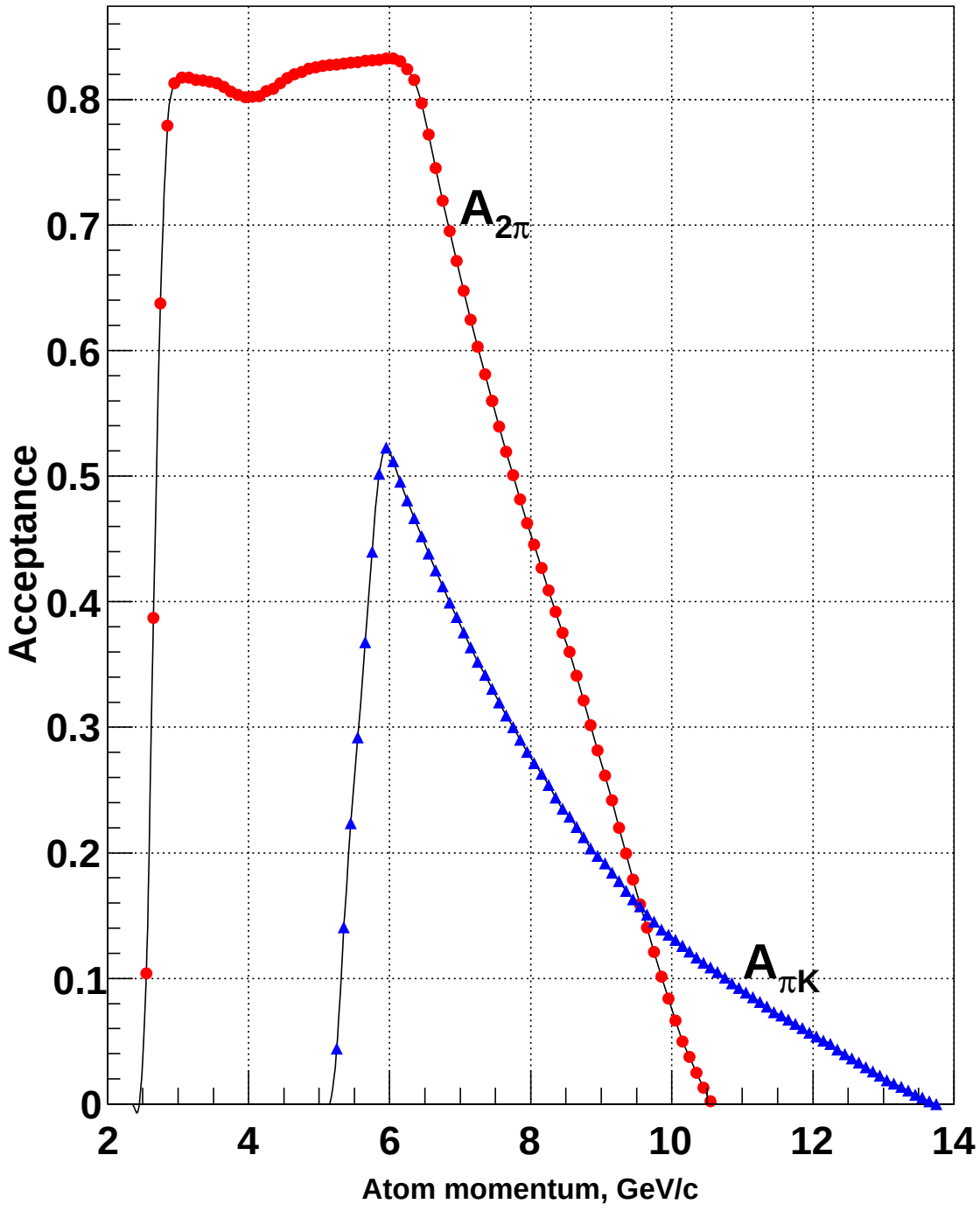

Figure 18: The acceptance behavior of DIRAC setup for case of $A_{2\pi}$ and $A_{\pi K}$ atoms. The decays of pions and kaons are not taken into account.

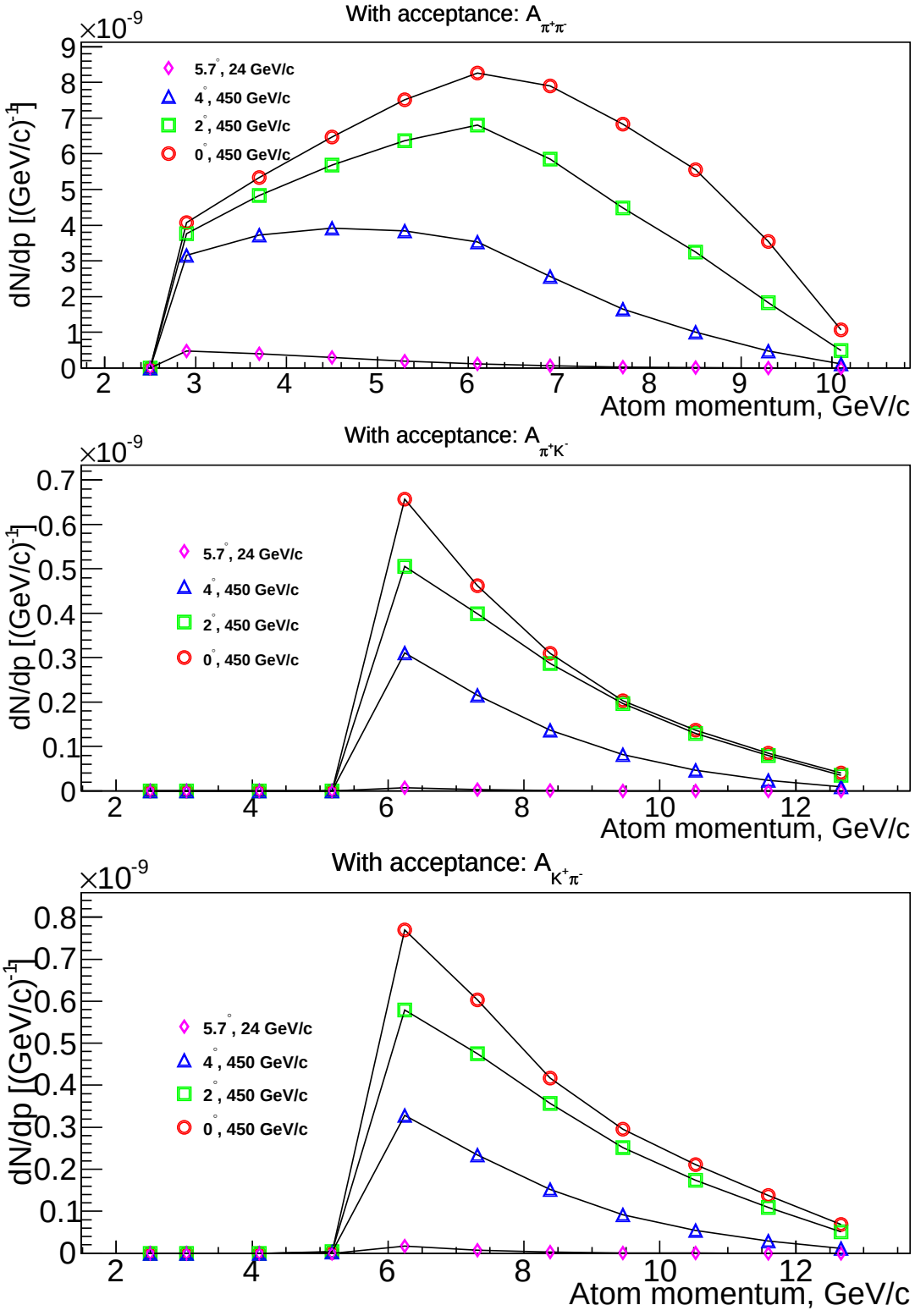

Figure 19: Yields of $A_{2\pi}$, $A_{\pi K}$ and $A_{K\pi}$ atoms per one p-Ni interaction at the proton momentum 450 GeV/c and emission angles $\theta_{lab} = 0°$, $2°$, $4°$ and at the proton momentum 24 GeV/c and emission angle $\theta_{lab} = 5.7°$ as a function of the atom momentum in l.s. for solid angle of 10^{-3} sr. The acceptance of the DIRAC setup is taken into account.

References

[1] J.Uretsky and J.Palfrey, Phys. Rev. **121** (1961) 1798.

[2] S.M.Bilenky et al., Yad. Phys. **10** (1969) 812; (Sov. J. Nucl. Phys. **10** (1969) 469).

[3] J. Gasser et al., Phys. Rev. **D64** (2001) 016008; he*p*-ph/0103157.

[4] J.Schweizer, Phys. Lett. **B587** (2004) 33

[5] B.Adeva at al., Phys. Lett. **B619** (2005) 50.

[6] A.Adeva et al.,Phys. Lett. **B704** (2011) 24.

[7] A.Adeva et al.,Phys. Lett. **B735** (2014) 288.

[8] P.Buttker, S.Descotes-Genon, B.Moussallam, Eur. Phys. J. **c33** (2004) 409. J. High Energy Phys. **O405**(2004) 036 he*p*-ph/0404150 .

[9] V.Bernard et al., Nucl. Phys. **B357** (1991) 129., Phys. Rev. **D43** (1991) 3557.

[10] J.Bijnens et al., J. High Energy Phys. **O405**(2004) 036 hep-ph/0404150 .

[11] C.B.Lang, et al., Phys. Rev. **D86** (2012) 054508.

[12] L.Nemenov, Yad. Fiz. **41** (1985) 980.

[13] L.L.Nemenov and V.D.Ovsiannikov, Phys. Lett. **B514** (2001) 247.

[14] L.L.Nemenov, V.D.Ovsyannikov, E.V.Chaplygin, Nucl. Phys. **A710** (2002) 303.

[15] J.R.Bateley at al., Eur. Phys. J. **C64** (2009) 589.

[16] J.R.Bateley at al., Eur. Phys. J. **C70** (2010) 635.

[17] To be published.

[18] O.E.Gorchakov et al., Yad. Fiz. **59** (1996) 2015;(Phys. At. Nucl. **59** (1996) 1942).

[19] O.E.Gorchakov et al., Yad. Fiz. **63** (2000) 1936;(Phys. At. Nucl. **63** (2000) 1847).

[20] O.Gorchakov and L.Nemenov[JINR], DIRAC Note **2012-6**.

[21] Sjöstrand T., Bengtsson M., Com. Phys. Comm. **43** (1987) 367.

[22] V.Uzhinsky, arXiv:1109.6768[hep-ph], 2011.

[23] S. Agostinelli et al., NIMPA **506** (2003) 250.

[24] N.Abgrall at al , Phys.Rev C84 034604(2011), Phys.Rev. **C85** 035210(2012), Private communication.

[25] G.Ambrosini at al.,Eur.Phys.J. **C10** (1999) 605.

[26] D.S.Barton at al.,Phys. Rev. **D27** (1983) 2580.

[27] Grishin V.G., Inclusive processes in hadron interactions at high energy. Energoizdat, Moscow 1982, p. 131 (in Russian).

[28] Eichten T. et al., Nucl. Phys. **B44** (1972) 333.

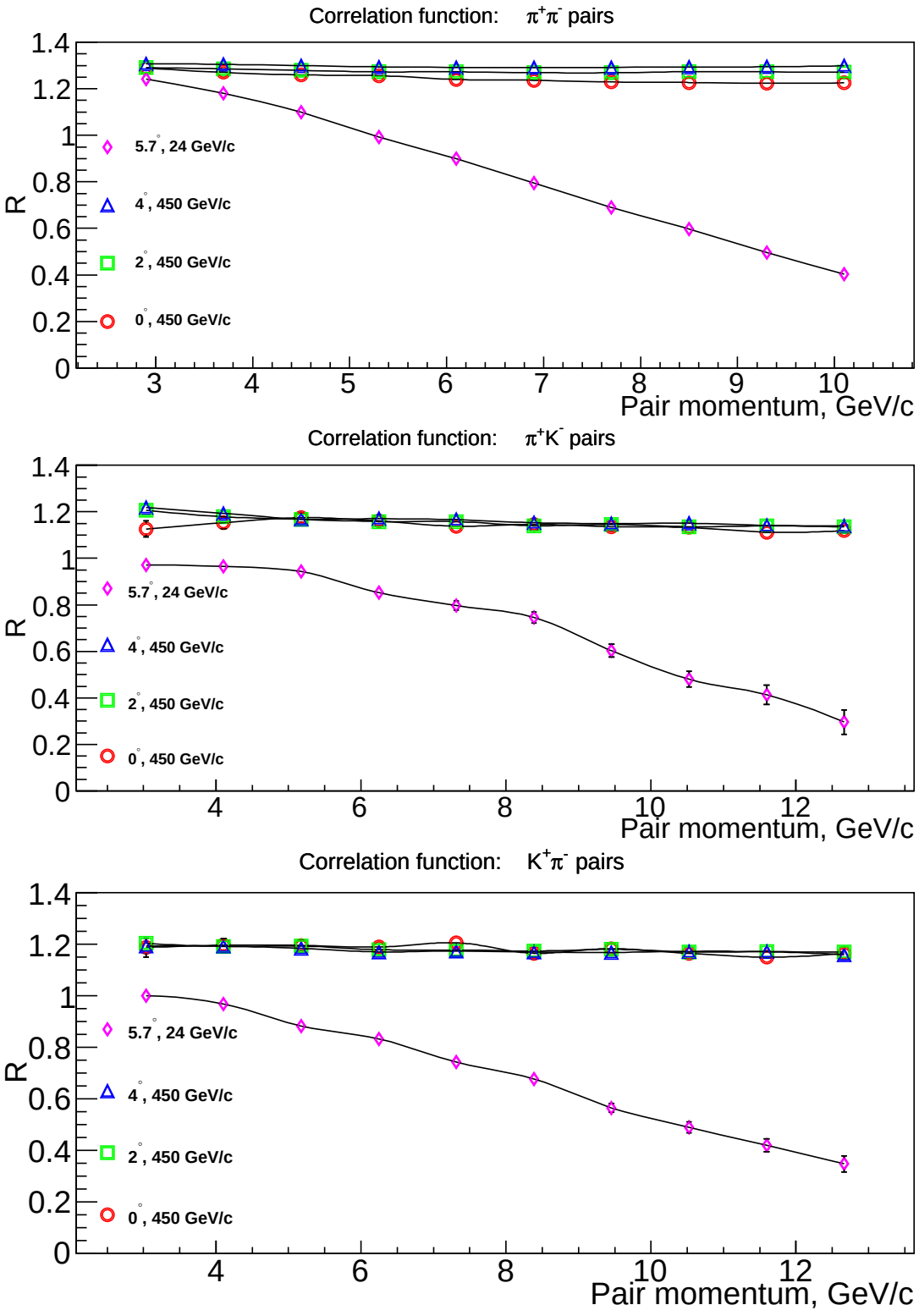

Figure 20: The dependence of correlation factor R for $\pi^+\pi^-$, π^+K^- and $K^+\pi^-$ pairs in the DIRAC setup on their momentum in l.s. for the proton momentum 450 GeV/c and emission angles $\theta_{lab} = 0°$, $2°$, $4°$ and at the proton momentum 24 GeV/c and emission angle $\theta_{lab} = 5.7°$.